Multipulse NMR spectroscopy

L. M. Soroko

Joint Institute for Nuclear Research, Dubna, Moscow District

Usp. Fiz. Nauk **156**, 653–682 (December 1988)

Multiquantum coherence and multidimensional homonuclear NMR spectroscopy are reviewed. Various types of multipulse spectroscopy are described: shift correlation spectroscopy (COSY), relayed shift correlation spectroscopy (RCOSY), multiquantum spectroscopy, spin-echo spectroscopy (SECSY), and spectroscopy based on the Overhauser effect (NOESY). Two-dimensional *J*-spectra, zero-quantum 2D spectra, and methods for obtaining 3D NMR and ACCORDION spectra are also described. The review ends with a brief description of new methods of 1D NMR spectroscopy. The discussion is carried out in terms of spin product operators.

CONTENTS

1. INTRODUCTION

Nuclear magnetic resonance (NMR) arises for nuclei with nonzero spins. This phenomenon can be observed if a test sample is placed in a uniform magnetic field and subjected to a radio-frequency (rf) magnetic field. Although NMR is associated with the internal mechanical and magnetic moments of a nucleus and is of a quantum-mechanical nature, classical models are frequently valid for describing it. For example, if the nuclear spin is 1/2, and if the spins are coupled only weakly with neighboring spins and with the lattice of the sample, a graphic vector model is sufficient for describing many (but not all!) methods of NMR spectroscopy.

The static magnetic field is required in NMR spectroscopy so that the sample will acquire an induced macroscopic magnetization. This magnetization is directed along the field lines of the static field and is proportional to the magnetic induction at the position of the sample. The macroscopic magnetization of the sample persists as long as there is a magnetizing magnetic field or until the system of nuclear spins is removed from it by the flow of a liquid or by a mechanical motion of the sample. However, only the transverse component of the magnetization vector of the sample is directly observable in NMR spectroscopy. In a steady state, this transverse component is zero. In order to create such a component, one "irradiates" the sample with a short pulse of a resonant rf field, which is directed perpendicular to the macroscopic magnetization vector of the sample (Fig. 1a). The amplitude and duration of the rf field pulse are chosen such that the magnetization vector of the sample after the rf pulse is rotated through 90° in the rotating coordinate system. The transverse magnetization of the sample which is produced with the help of the $\pi/2$ pulse of rf field precesses in the magnetic field at resonance frequencies and induces an emf in an induction coil which either completely surrounds the test sample or is positioned near the irradiated region. The NMR spectrum of a given spin is found by using Fourier transforms to carry out a spectral-frequency analysis of the emf signal $s(t)$, which decays with a relaxation time of 10^{-2}–10^{2} s. Each spectral line in the NMR spectrum, with a frequency ω_0, makes a contribution

$$s(t) = \exp(i\omega_0 t) \exp\left(-\frac{t}{T_2}\right), \tag{1}$$

to the emf signal, where T_2 is the spin-spin relaxation time. The profile of the line is described by

$$S(\omega) = A(\omega) + iD(\omega). \tag{2}$$

It consists of an absorbing component (or mode)

$$A(\omega) = \frac{T_2}{1+T_2^2(\omega-\omega_0)^2}, \tag{3}$$

which is the real part of the spectrum, and a dispersive component (or mode)

$$D(\omega) = \frac{T_2^2(\omega-\omega_0)}{1+T_2^2(\omega-\omega_0)^2}, \tag{4}$$

which is the imaginary part of the spectrum. There are three basic ways in which an NMR spectrum is displayed: 1) in the purely absorbing mode, $A(\omega)$; 2) in the purely dispersive mode, $D(\omega)$; and 3) as a power spectrum

$$P(\omega) = |A(\omega)|^2 + |D(\omega)|^2, \tag{5}$$

which is called the "absolute value mode."

Each spectral line in an NMR spectrum has a chemical shift: the relative difference between the precession frequen-

 0038-5670/88/121043-17$01.80

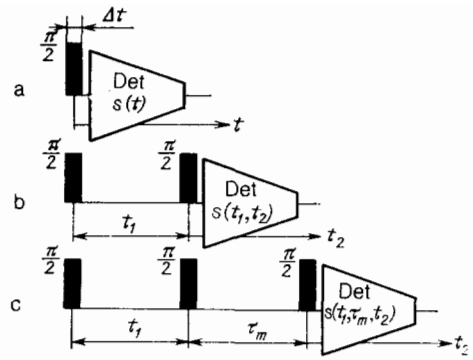

FIG. 1. Trains of rf field pulses used in modern nuclear-magnetic-resonance (NMR) spectrometers. a—A single $\pi/2$ pulse of length Δt creates a transverse magnetization of spins in the frequency interval $\Delta\omega \approx (4\Delta t)^{-1}$ near the resonance frequency; b—Two $\pi/2$ pulses, separated in time, are used to produce a 2D NMR spectrum; c—a train of three $\pi/2$ pulses in systems for observing multiquantum coherence and multiquantum transitions in NMR spectra. Det—The stage in which the NMR signals are detected.

cies of the free spin and of the spin bound in the given chemical compound. The spectrum of chemical contains information about the structure of the molecules and about the interaction of like or different spins in different parts of a molecule. In a solid, the chemical shifts depend on the angular orientation of the molecule with respect to the external magnetic field and are characterized by the principal values of the chemical-shift tensor. In an amorphous solid or a powdered sample an NMR spectral line is greatly spread out and has a distinctive "powder" structure.

Spins with a low gyromagnetic ratio and a small natural isotopic concentration, e.g., ^{13}C and ^{15}N, generate weak NMR signals. In order to amplify these signals and thus reduce the time required to measure the NMR spectra of such spins (which sometimes reaches 10–20 h), the sample is subjected to rf fields at two resonant frequencies: at the precession frequency of an abundant spin (I) and at the precession frequency of the low-abundance spin (S), with which spin I is coupled. The difference between the gyromagnetic ratios of the spins I and S is canceled out by choosing the amplitudes of the rf fields in inverse proportion to the corresponding gyromagnetic ratios. When these conditions are met, the magnetization of spin I is transferred to spin S.

The interaction energy of two spins in the same molecule depends on the relative orientation of these spins. For this reason, the spectrum of chemical shifts consists of multiplets, which are superimposed on each other. As a result, interpreting the spectral information becomes difficult or ambiguous. The situation can be changed if the hyperfine splitting in the multiplets is eliminated by a decoupling method. For this purpose, during the recording of the emf signal from the first spin the second spin is irradiated with an rf field of higher power. The second spin precesses rapidly, and a dynamic averaging of the interaction of the two spins sets in. The multiplets shrink to singlets. A similar averaging of spin interactions occurs in a liquid during rapid and random translational and rotational motions of the molecules. The spectrum of chemical shifts in a liquid thus consists of narrow resonance lines. In solids, on the other hand, there are no natural processes which act to average out the spin interactions. As a result, the width of the resonance NMR lines is 10^3–10^5 times that in a liquid. In order to reduce the width of the NMR spectral lines in a solid, one rotates the sample rapidly at the magic angle $\theta =$ across $\sqrt{1/3} \approx 54°44'$ with respect to the main magnetic field, or one applies to the sample a train of shirt rf pulses which cause the magnetization vector to become oriented alternately along each of the three mutually orthogonal axes of the rotating coordinate system. The spin interactions, which are caused in this case by the dipole-dipole interaction of the nuclear magnetic moments, are averaged out, and the width of the resonances in the NMR spectrum in the solid is reduced by a factor of 10–100.

In order to obtain more-comprehensive information about the interaction of spins in a molecule and thus about the structure of the molecule, one applies two rf pulses to the sample at the resonance frequency of the spin of interest, in such a way that the two pulses are separated in time. Each rf field pulse rotates the magnetization vector through an angle of 90° (a $\pi/2$ pulse; Fig. 1b). At the time at which the second rf field pulse is applied, the components of the magnetization vector which are precessing at different frequencies and which have different chemical shifts are not in phase, as they are just after the first $\pi/2$ rf pulse. Accordingly, NMR signals which are measured with different time intervals between the two $\pi/2$ rf pulses differ from the NMR signal which is measured directly after the first $\pi/2$ rf pulse. The 2D data file on $s(t_1,t_2)$ is subjected to spectral analysis and converted into a 2D spectrum $S(\omega_1,\omega_2)$, in which the chemical-shift effect is separated from the spin-interaction effect. The structure of each spectral line in a 2D NMR spectrum

$$S(\omega_1, \omega_2) = (A(\omega_1) A(\omega_2) - D(\omega_1) D(\omega_2)) - i(A(\omega_1) D(\omega_2) + D(\omega_1) A(\omega_2)), \quad (6)$$

however, is of such a nature that neither its real part nor its imaginary part is purely absorbing or purely dispersive. In order to represent the 2D NMR spectrum in a pure mode, one measures two or more independent signals $s(t_1,t_2)$, varying (for example) the orientation of the initial magnetization vector after the first $\pi/2$ rf pulse.

The 2D NMR spectra contain so-called cross peaks with $\omega_1 \neq \omega_2$, which contain information on which spins in the molecule are coupled with each other and also on the distances separating these spins in the given molecule.

Experiments carried out to observe multiquantum coherence and multiquantum transitions can be judged the most interesting experiments in high-resolution NMR spectroscopy. Multiquantum transitions arise when a spin system consists of two or more coupled spins with a spin of 1/2 or when the spin of a resonating nucleus satisfies $I \geqslant 1$. In these experiments, the sample is subjected to three rf field pulses (Fig. 1c). The first of these pulses creates the initial transverse magnetization of the sample, as usual. During the evolution stage, the different components of the magnetization vector precess at different frequencies. The second rf pulse (the "mixing pulse") puts the magnetization of the sample in a state with a multiquantum coherence, which is not directly observable after the second rf pulse. After the third rf pulse, the multiquantum coherence then becomes a single-quantum coherence. The NMR signals are measured

with various time intervals between the second and third rf pulses.

Multiquantum coherence has the following important properties: If the frequency of the carrier oscillations of the electromagnetic field in the rf field pulse is separated from the center of the resonance line, the signals with a p-quantum coherence experience a detuning which is p times that for single-quantum signals. A phase shift of $\Delta\varphi$ of the carrier in the rf field pulse is observed in signals with a p-quantum coherence as a phase shift of $p\Delta\varphi$. Finally, if a linear field gradient G is imposed on the main magnetic field, a signal with a p-quantum coherence will be subjected to an effective magnetic field gradient which is p times the actual gradient. In particular, the effect of a variation in the magnetic field is not seen at all in signals with a zero-quantum coherence. From an NMR signal which contains several components of a multiquantum coherence one can filter out an NMR signal with a given coherence p. The customary approach in NMR spectroscopy is to use methods to form a zero-quantum and two-quantum coherence, particularly in a study of a system of two spins. The maximum number of quanta which have been observed in multiquantum experiments in a solid is about 100.

In a uniform magnetic field, one usually studies samples which have a homogeneous structure. If the sample is instead inhomogeneous, one will detect a set of NMR signals, each corresponding to a small part of the sample. In such a situation one uses a gradient of the magnetic field and spatially selective rf field pulses in the presence of a magnetic field gradient; alternatively, one uses surface induction coils which are spatially selective.

Methods of NMR spectroscopy are widely used in organic chemistry, biophysics, biochemistry, and medicine. Nuclear-magnetic-resonance spectroscopy competes successfully with the methods of x-ray structural analysis in research on polycrystalline samples. The NMR phenomenon is utilized in radiationless tomography (NMR subsurface imaging) to generate anatomical and biochemical images of the head and internal organs of humans and for microscopy of cells.

The "spin industry" now includes tens of large companies and about a hundred research institutes, which are developing new methods of NMR spectroscopy and which are also producing NMR equipment and dedicated computers. Today's NMR spectrometers, equipped with superconducting or resistive electromagnets, generate high- and ultrahigh-resolution NMR spectra, both 1D and 2D. Apparatus is being manufactured to rotate a sample rapidly at the magic angle and to irradiate solids with multipulse rf field trains. Experiments with multiquantum coherence which investigate pairings of ^{13}C nuclei in organic molecules and also the diffusion of molecules have become conventional. Finally, several types of NMR subsurface imaging apparatus have been developed and tested successfully for producing NMR images, for visualizing liquid flows (in particular, the motion of blood in human blood vessels), and for generating localized high-resolution NMR spectra. The scale of the effort can be seen from the fact that no less than two billion dollars was devoted to the manufacture of NMR imaging equipment in the US in 1986.[1] Methods of NMR spectroscopy have acquired much practical importance, and the number of specialists who have become part of the "spin industry" at various stages of the development and use of NMR equipment is constantly growing. The present review, which may be thought of as a supplement to the monographs of Refs. 2 and 3, is devoted to multiquantum coherence and multidimensional homonuclear NMR spectroscopy. The physical and mathematical foundations of the most typical methods of modern NMR spectroscopy are presented using the example of two-spin systems. This review does not cover the problems of the analysis of heterogeneous or multispin systems or the use of these methods to analyze the structure of complex molecules in liquids.

2. MULTIQUANTUM COHERENCE

A system of several interacting spins goes into a state with a transverse magnetization after the first $\pi/2$ rf field pulse. This state is a coherent state, since all the spins are precessing at the same initial phase, for example, from a position in which the transverse magnetization vector of the sample is directed along the y axis in the rotating coordinate system. The coherence is not lost in the stage of evolution after the first $\pi/2$ rf pulse, in which the spins precess at different frequencies in accordance with the chemical shifts. According to the quantum-mechanical treatment, the NMR signal detected after the end of the first $\pi/2$ rf pulse corresponds to single-quantum transitions between energy levels of the spin in the static magnetic field. The difference between the magnetic quantum numbers of these levels before and after this transition, m_{init} and m_{fin}, obeys the conditions $\Delta M = m_{\text{init}} - m_{\text{fin}} = \pm 1$.

Under the influence of the chemical shift at the frequency Ω, the x and y components of the magnetization vector I evolve freely after the $\pi/2$ rf field pulse, rotating in the xy plane of the rotating coordinate system[4]:

$$\begin{aligned} I_x &\xrightarrow{\Omega t I_z} I_x \cos\Omega t + I_y \sin\Omega t, \\ I_y &\xrightarrow{\Omega t I_z} I_y \cos\Omega t - I_x \sin\Omega t, \end{aligned} \tag{7}$$

where t is the time which has elapsed after the $\pi/2$ rf pulse. After the second $\pi/2$ rf pulse, the system of spins goes into a state with a multiquantum coherence. This state is coherent, as is the macroscopic magnetization of the sample, which begins its evolution after the first $\pi/2$ rf pulse. The state with multiquantum coherence, however, cannot be reduced to a magnetization of the sample, since in this state there are components of quantum-mechanical transitions with $\Delta M = m_{\text{init}} - m_{\text{fin}} \neq \pm 1$, e.g., $\Delta M = 0$ or $\Delta M = \pm 2$. The multiquantum coherence formed after the second $\pi/2$ rf pulse does not contribute to the NMR signal detected after the second $\pi/2$ rf pulse. The task of a researcher carrying out NMR experiments with a multiquantum coherence is to form a state of a system of several spins with a given multiquantum coherence and then, after the evolution stage, to use a detecting rf pulse to transform this coherence into an observable single-quantum coherence. A third $\pi/2$ rf pulse is ordinarily used for this transformation, along with a certain programmed alternation of phases of the rf pulses and of a reference signal in the receiver, followed by an averaging of the file of the measured NMR signals.

In a system consisting of two spins A and X with values of 1/2, two types of single-quantum coherence arise. Correspondingly, two types of transverse magnetization of the sample arise[4]: an in-phase transverse magnetization, with

the magnetization vectors of A and X parallel to each other, and an out-of-phase (or antiphase) transverse magnetization, with these vectors being antiparallel to each other (Fig. 2). The out-of-phase magnetization of spin A is nonzero when the energy levels of spin X have unequal populations, e.g., when the A, X spin system is at thermal equilibrium. The in-phase magnetization of spin A is described by the component $I_x^{(A)}$ of the vector $\mathbf{I}^{(A)}$, while the out-of-phase magnetization is described by a product of components of the vectors $\mathbf{I}^{(A)}$ and $\mathbf{I}^{(X)}$ of the type $2I_x^{(A)}I_z^{(X)}$ (Ref. 6). After a time interval $\tau = (2J)^{-1}$ where J is the constant of the scalar coupling of the interacting spins A and X, the in-phase x magnetization of spin A becomes an out-of-phase y magnetization.

The process by which the in-phase x magnetization in the A, X spin system transforms into an out-of-phase y magnetization under the influence of the scalar spin-spin coupling is described by the expression

$$I_x^{(A)} \xrightarrow{\pi J\tau \cdot 2I_z^{(A)}I_z^{(X)}} I_x^{(A)} \cos \pi J\tau + 2I_y^{(A)}I_z^{(X)} \sin \pi J\tau. \qquad (8)$$

The transition of the in-phase y magnetization into the out-of-phase x magnetization is described by

$$I_y^{(A)} \xrightarrow{\pi J\tau \cdot 2I_z^{(A)}I_z^{(X)}} I_y^{(A)} \cos \pi J\tau - 2I_x^{(A)}I_z^{(X)} \sin \pi J\tau. \qquad (9)$$

The corresponding processes by which the out-of-phase magnetization transforms into an in-phase magnetization are described by

$$\begin{aligned} 2I_x^{(A)}I_z^{(X)} &\xrightarrow{\pi J\tau \cdot 2I_z^{(A)}I_z^{(X)}} 2I_x^{(A)}I_z^{(X)} \cos \pi J\tau + I_y^{(A)} \sin \pi J\tau, \\ 2I_y^{(A)}I_z^{(X)} &\xrightarrow{\pi J\tau \cdot 2I_z^{(A)}I_z^{(X)}} 2I_y^{(A)}I_z^{(X)} \cos \pi J\tau - I_x^{(A)} \sin \pi J\tau. \end{aligned} \qquad (10)$$

The two-quantum (DQC) and zero-quantum (ZQC) coherences in a system of two spins A and X are described by products of the type I_xI_y, I_xI_x, and I_yI_y. A pure multiquantum coherence corresponds to a linear combination of these products. Under the influence of the sum of the chemical shifts in the system of two spins A,X the components of a pure two-quantum coherence and of a pure zero-quantum coherence evolve at frequencies which are respectively equal to the sum and difference of the chemical-shift frequencies Ω_A and Ω_X.

In order to detect a two-quantum coherence in a spin system A, X, one irradiates spin X with a $\theta(x)$ pulse of an rf field at a time t_2 after the second $\pi/2$ (y) rf pulse; after a time interval $(2J)^{-1}$, one begins to detect the NMR from spin A. The rf pulse $\theta(x)$ rotates the magnetization I_x^X through an angle of θ radians. The two-quantum coherence transforms in accordance with

$$2I_y^{(X)}I_x^{(A)} \xrightarrow{\theta(X)(x)} 2I_y^{(X)}I_x^{(A)} \cos \theta + 2I_z^{(X)}I_x^{(A)} \sin \theta. \qquad (11)$$

The first term in (11) corresponds to a weakened and still unobservable two-quantum coherence. The second term represents the out-of-phase magnetization of spin A, which transforms over a time $(2J)^{-1}$ into an in-phase magnetization $I_y^{(A)} \sin \theta$. To produce an NMR signal of maximum amplitude, one chooses the angle θ, through which the spin is rotated in the third rf pulse, to be equal to $\pi/2$ radians. In an A,X spin system with a scalar coupling, the NMR signal does not depend on the duration of the evolution stage, t_2, since the two-quantum coherence D_0 which is the only one that exists in this stage does not evolve between the second and third rf pulses.

A train of rf pulses which is symmetric with respect to excitation and detection (Fig. 3) is used for the uniform excitation of multiquantum coherence and detection of the NMR spectra in some one mode.[7,27] The first part of the train is the same as the standard pulse train a. At point 1 of train a, after a $\pi/2(x)$ rf pulse, a transverse magnetization arises: $-(I_y^{(A)} + I_y^{(X)})$. By the end of the evolution stage, at point 2, this magnetization reaches a state

$$\sigma_2 = (I_y^{(A)} + I_y^{(X)}) \cos \pi J\tau - (2I_x^{(A)}I_z^{(X)} + 2I_z^{(A)}I_x^{(X)}) \sin \pi J\tau. \qquad (12)$$

The chemical-shift effects are suppressed in this state by the first π pulse. The second $\pi/2(x)$ rf pulse transforms the second term in (12) into a pure two-quantum coherence $(\mathrm{DQC})_y$ at point 3:

$$\sigma_3 = (2I_x^{(A)}I_y^{(X)} + 2I_y^{(A)}I_x^{(X)}) \sin \pi J\tau. \qquad (13)$$

The effect of the first term in σ_3 is eliminated by an alternation of the phases of the rf pulses.

An important feature of expression (13) is that the magnitude of the pure two-quantum coherence, σ_3, depends on the preparation time τ through $\sin \pi J\tau$, which does not allow averaging over the many times τ which would be required for the uniform excitation of a multiquantum coherence. After the detection of the $\pi/2(x)$ rf pulse at point 4, an out-of-phase magnetization arises:

$$\sigma_4 = (2I_x^{(A)}I_z^{(X)} + 2I_z^{(A)}I_x^{(X)}) \sin \pi J\tau. \qquad (14)$$

by the end of the stage of free precession, of length τ, this magnetization reaches the state[7]

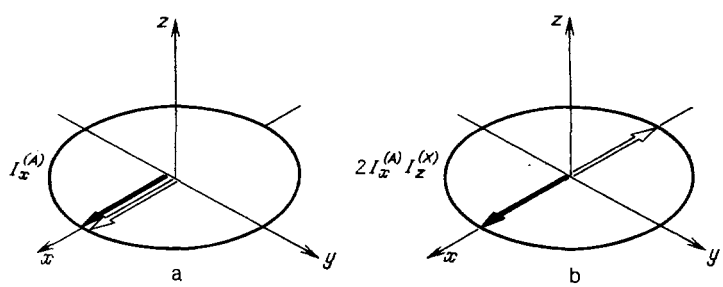

FIG. 2. Vector model used to explain the difference between the (a) in-phase and (b) out-of-phase magnetizations of a sample in a system of two coupled spins A and X.

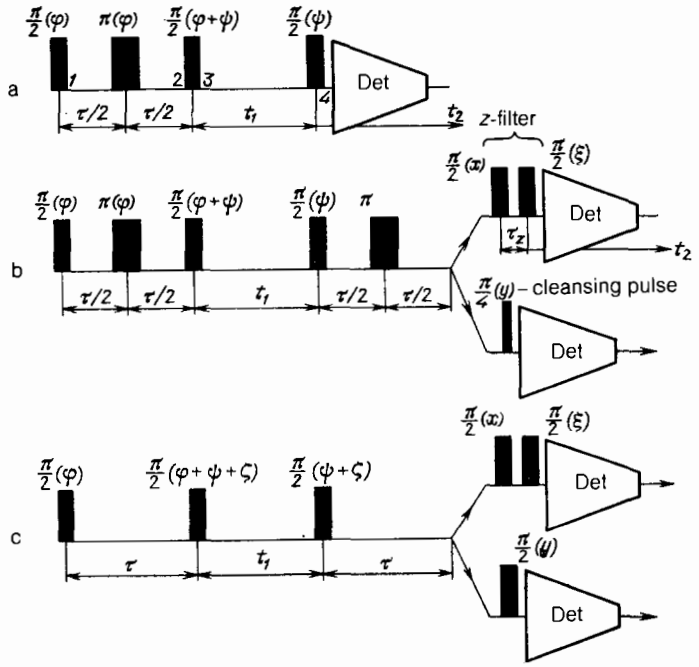

FIG. 3. Train of rf field pulses used for the uniform excitation of multiquantum coherence and to produce NMR spectra without phase distortions. a—Standard train of rf field pulses for the excitation of a p-quantum coherence [here $\varphi = k\pi/p$ ($k = 0,1,2,\ldots 2p-1$), and the signs of the NMR signals are alternated in turn during the data acquisition]; b—train of rf field pulses which are symmetric with respect to excitation and detection (a cleansing rf pulse or z-filter is used in this trains); c—equivalent train of rf field pulses in which there is no refocusing π pulse, and the phase ξ is alternated in accordance with $\xi = 0$, $\pi/2$.

$$\sigma_5 = -(2I_x^{(A)}I_z^{(X)} + 2I_z^{(A)}I_x^{(X)})\sin\pi J\tau$$

$$\times\cos\pi J\tau - (I_y^{(A)} + I_y^{(X)})\sin^2\pi J\tau. \qquad (15)$$

After an average is taken over the variable τ, we are left with only an out-of-phase magnetization

$$\sigma_5^{\text{avg}} = -\frac{1}{2}(I_y^{(A)} + I_y^{(X)}), \qquad (16)$$

which does not depend on the coupling constant J. It has been shown[7] that a corresponding averaging process makes it possible to arrange a uniform excitation of a p-quantum coherence in a system of N spins with a value of 1/2. The primary distinctive feature of the train in Fig. 3b is that the third (detecting) $\pi/2$ rf pulse "scatters" the multiquantum coherence in the form of a transverse out-of-phase magnetization uniformly among the p active spins. To suppress the contributions of the out-of-phase magnetization in the stage in which the NMR signal is detected, a "cleansing" $\pi/2$ (y) pulse is introduced in each even-numbered experiment, just before the beginning of the detection of the NMR signal.[7] In a system consisting of two spins A, X, the $\pi/2$ (y) cleansing pulse changes the sign of the first term of state σ_5 in (15). If the even-numbered experiments are taken with a plus sign, and the odd-numbered ones with a minus sign, this term will disappear when an average is taken over many NMR signals.

In a corresponding way, one constructs a train of rf pulses in multiquantum filters. For example, if we wish to excite only the p-quantum coherence we would use the train in Fig. 3c. The phase φ of the first $\pi/2$ pulse and of the first π pulse is changed $2p$ times: $\varphi = k\pi/p$, $k = 0,1,\ldots,2p-1$. The even-numbered NMR signals are taken with a plus sign, and the odd-numbered ones with a minus sign. The phase ψ of the second and fourth $\pi/2$ pulses is taken to be 0 for even p or $\pi/2$ for odd p.

There are several techniques for arranging a spectral separation or spacing of the NMR of overlapping or adjacent lines of multiquantum transitions.[11] The direct method of tuning the reference signal away from the center of the NMR signal has not been adopted widely because in systems in which a spin-echo signal is formed in the evolution stage the frequency-separation effect disappears at the same time as the effect of the variation in the magnetic field is established. Accordingly, one introduces phase shifts of the rf field in a preparation stage. The signal representing the p-quantum transition undergoes a phase shift which is p times the original shift. In order to separate the multiquantum transitions which are marked with different phase shifts one alters the phase of the rf field, φ, $(2p_{\max}+1)$ times in the interval between the values of 0 and 2π radians, where $p_{\max}$ is the greatest order of the coherence in the NMR spectrum. The 2D data file is subjected to not only the standard Fourier transform in the variable t but also to a discrete Fourier transform in the variable φ. As a result, the coordinate φ is converted into the conjugate coordinate p.

In a method for separating multiquantum transitions which has been adopted widely the phase of the rf field in the preparation stage, φ, is increased monotonically with the duration of the evolution stage, t_1: $\varphi = \Delta\omega\cdot t_1$, in steps of $\Delta\varphi = \Delta\omega\cdot\Delta t_1$. The separation of the multiquantum transitions occurs after discrete Fourier transforms in the variable t_1 are taken.[11] In contrast with the preceding method, the separation of the multiquantum transitions occurs in a single measurement, precisely as in a direct method with a frequency difference. If all the multiquantum transitions up to $p_{\max}$ are to be represented without an overlap, the increment Δt_1 in the evolution stage must be reduced by a factor of at least $(2p_{\max}+1)$.

The refocusing π pulse, introduced in the evolution stage, can be used to separate multiquantum transitions by a phase-shift method. In this approach, the phase of the rf field of the π pulse is altered sequentially, from experiment to experiment. Each p-quantum transition acquires a phase shift larger by a factor of $2p$ than the initial shift. The additional factor of 2 arises here because the π pulse causes a transfer of coherence from the $+p$ state to the $-p$ state. Multiquantum transitions can be marked on the basis of the

angle of the rotation around the z axis with the help of composite pulses.[12] Finally, a pulse p of a given resonance line in the original NMR spectrum can be identified "passively," on the basis of the width of the spectral line in a nonuniform magnetic field, which increases linearly with p.

Spatial variations in the magnetic field do not influence zero-quantum coherence. Accordingly, a spectrum with a zero-quantum coherence has a high resolution ($\approx 10^{-10}$) without the assistance of refocusing π pulses of an rf field. Another interesting point is that zero-quantum coherence can be excited and detected without the help of any rf pulses.[11] For this purpose, one sends the spin system from one state to another rapidly enough that the initial and final Hamiltonians, $\mathscr{H}_{\text{init}}$ and $\mathscr{H}_{\text{fin}}$, do not commute with each other. The off-diagonal elements of the density matrix, σ_{kj} ($k \neq j$), then acquire oscillatory factors $\exp(-i\omega_{jk}t)$, as during the application of an rf pulse. For example, zero-quantum coherence arises under conditions such that reacting spins A and X are strongly coupled. A difference in magnetization arises if the chemical components are placed in a magnetic field just before they are mixed. Under these conditions, zero-quantum coherence arises essentially instantaneously, and there is no need for a preparatory stage.[67]

The sequence of events in multipulse experiments can be described in a graphic way by means of a coherence-transfer diagram (Fig. 4).[8] Transitions between diagram levels (not between energy levels!) with different values of p occur only during the application of rf pulses, and they cannot occur in the stage of free precession. All paths on the coherence-transfer diagram begn at diagram level $p = 0$ and end at diagram level $p = -1$.

Coherence-transfer diagrams make it possible to interpret clearly various types of 2D NMR spectroscopy.[8] For example, corresponding to 2D single-quantum homonuclear correlation spectroscopy (2D COSY) using a train of two rf pulses,

$$\frac{\pi}{2}(x) - t_1 - \beta(\varphi) - t_2 - \text{detection of data},$$

there are two coherence-transfer paths: $[p = 0] \rightarrow [\pm 1] \rightarrow [-1]$. In exchange spectroscopy (2D NOESY) with three rf pulses, two coherence-transfer paths arise: $[p = 0] \rightarrow [\pm 1] \rightarrow [0] \rightarrow [-1]$. The coherence-transfer paths in relayed shift correlation spectroscopy (2D RCOSY) and also in two-quantum correlation spectroscopy (COSY $\oplus$ DQC filter) have the form (Fig. 4, b and c) $[p = 0] \rightarrow [\pm 1] \rightarrow [+2] \rightarrow [-1]$. Coherence-transfer diagrams make it possible to interpret known pulse sequences and to synthesize new ones in multipulse experiments. The coherence-transfer diagrams discussed above are once again a clear demonstration that the program of alternation of the phases of the rf pulses is the main consideration in the selection of a certain coherence-transfer path. It was in this manner that it was discovered that experiments with four rf pulses could be replaced by equivalent three-pulse experiments.

Multiquantum NMR spectroscopy in solids has some fundamentally new features.[5,9,10] In contrast with molecules in a liquid, which usually contain a small number of interaction spins, and in which case the NMR spectra which are recorded are characterized by a small value of $p_{\max}$, in a solid there are dipole-dipole bonds spanning large groups of spins (clusters). The number of multiquantum transitions increases under these conditions to the extent that individual spectral lines merge into unresolved bands. The subject observed in corresponding multiquantum experiments becomes, for example, the dependence of the intensity of multiquantum bands on the value of p, rather than the individual spectral lines. Because of the destructive interference of the spectral components within each band, however, the intensity of the latter becomes very low. In an effort to prevent this destructive interference, multiquantum coherence in a solid is excited by repeated sequences of short, powerful rf pulses, which are characteristic of NMR spectroscopy in a solid. The condition of time reversal, under which it is possible to form a uniform spin echo, becomes important.

Figure 5 shows a train of rf pulses with time reversal, intended for experiments in a solid.[9] The stage of preparation and also of mixing contains trains of four pairs of $\pi/2$ pulses which repeat k times, with alternating orientations of the axes around which the magnetization vector is rotated in the rotating coordinate system: x, $-x$, $-x$, x. The time intervals between pairs of pulses are equal to Δ, while those between pulses within each pair are 2Δ. With this type of alternation of the phases of the rf pulses, each eight-pulse

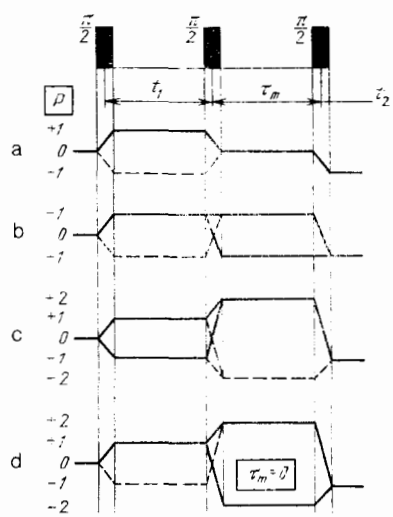

FIG. 4. Coherence-transfer paths in experiments with three rf pulses. a—2D NOESY; b—RCOSY; c—2D spectroscopy; d—COSY $\oplus$ DQC filter.

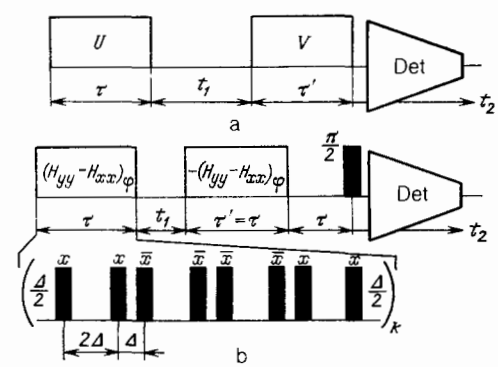

FIG. 5. Trains of rf pulses used in multiquantum spectroscopy of solids. a—Schematic diagram of a sequence of rf pulses containing a preparation stage of length τ with a propagator U, an evolution stage of duration t_1, a mixing state of duration τ' with a mixing propagator V, and a detection stage of duration t_2; b—train of rf pulses with time reversal: $U = V^+$.

train excites a two-quantum coherence. The orders with different values of p are separated under conditions of zero frequency difference by varying the phase of the rf pulses in accordance with $\varphi = \Delta\omega \cdot t_1$, while t_1 is varied simultaneously. The $\pi/2(x)$ detection pulse is applied 2 ms after the end of the mixing stage; then a spin-locking pulse 100 μs long is applied along the y axis. The phase of the $\pi/2(x)$ pulse is changed alternately by 180° in order to weaken the aritfacts caused by the unstable operation of the receiving apparatus.

It has been established[10] that coherences of progressively higher order appear gradually in the NMR spectras as the duration of the preparation stage, τ, is increased from 66 to 792 μs. In addition, the orders of the multiquantum coherence become redistributed, and the effective size of a cluster of interacting spins increases monotonically with τ. An important aspect of the dynamic process in which multiquantum coherence is excited within a cluster of spins in a solid is that this process is reversible and can be "refocused." For example, with $\tau = 528$ μs one observes a spectrum up to $p = 32$. If this time is changed from 66 to 462 μs, this multiquantum spectrum gradually shrinks to a two-quantum spectrum. It has thus been shown that the coherent evolution of a system with a large number of spins ($p \sim 100$) is reversible and that multiquantum phenomena in solids can be utilized as a method for counting the spins in a cluster.

3. MULTIDIMENSIONAL NMR SPECTRA[23]

3.1. Shift correlation spectroscopy (2D COSY). This spectroscopy version is based on the fundamental difference between the effects of chemical shifts (Ω) and of a scalar coupling of two spins (J). As can be seen from (7), the evolution under the influence of a chemical shift may be thought of as a rotation of the magnetization vector of spin A or X in the coordinate system (I_x,I_y) at an angular velocity Ω. Each of the operators of the sum $I_x^{(A)} + I_x^{(X)}$ or of the product $2I_x^{(A)}I_x^{(X)}$ of two noninteracting spins ($J = 0$) evolves independently under the influence of the chemical shifts Ω_A and Ω_X. We thus have

$$I_x^{(A)} + I_x^{(X)} \xrightarrow{\Omega_A t I_z^{(A)} + \Omega_X t I_z^{(X)}} (I_x^{(A)} \cos\Omega_A t + I_y^{(A)} \sin\Omega_A t) + (I_x^{(X)} \cos\Omega_X t + I_y^{(X)} \sin\Omega_X t), \quad (17)$$

$$2I_x^{(A)}I_x^{(X)} \xrightarrow{\Omega_A t I_z^{(A)} \cdot \Omega_X t I_z^{(X)}} 2(I_x^{(A)} \cos\Omega_A t + I_y^{(A)} \sin\Omega_A t) \times (I_x^{(X)} \cos\Omega_X t + I_y^{(X)} \sin\Omega_X t). \quad (18)$$

The evolution under the influence of a scalar coupling of two spins is different. It follows from (8) and (10) that the rotation of the magnetization vectors of spins A and X occurs in the coordinate system $I_x^{(A)}, 2I_y^{(A)}I_z^{(X)}$ (Fig. 6) and is accompanied by a transfer of coherence between the spins. The in-phase magnetization transforms into an out-of-phase magnetization, and then the out-of-phase magnetization changes back into an in-phase magnetization, but with the opposite sign.[4,13] This process repeats with a period $T = 2/J_{AX}$.

In 2D spectroscopy of the correlation of chemical shifts,[14] like spins A and X, e.g., protons, are subjected to two nonselected $\pi/2(x)$ rf field pulses (Fig. 7a). After the second $\pi/2(x)$ pulse, the state of a system with one-quantum coherence is described by an expression with four terms[4]:

$$\sigma_3 = (I_x^{(A)} \sin\Omega_A t_1 + I_x^{(X)} \sin\Omega_X t_1) \cos\pi J_{AX} t_1 \cdot - (2I_y^{(A)}I_z^{(X)} \sin\Omega_X t_1 + 2I_z^{(A)}I_y^{(X)} \sin\Omega_A t_1) \sin\pi J_{AX} t_1. \quad (19)$$

It can be seen from (19) that after the second $\pi/2(x)$ pulse the in-phase magnetization of the first spin, A, precesses at a frequency equal to the precession frequency of the second spin, Ω_X (!), and, on the other hand, the out-of-phase magnetization of the second spin, X, precesses at the precession frequency of the first spin, Ω_A. As a result, cross peaks appear in the 2D COSY spectrum.

The first term in (19) corresponds to a directly observable magnetization of spin A, which precesses at two frequencies: $\Omega_A + \pi J_{AX}$ and $\Omega_A - \pi J_{AX}$. The second term describes the magnetization of spin X, which precesses at two frequencies: $\Omega_X + \pi J_{AX}$ and $\Omega_A - \pi J_{AX}$. Because of the factor $\cos \pi J_{AX} t_1$, the first two terms contribute in-phase doublets which lie on the diagonal, and their centers are at the point with the frequencies $\omega_1 = \omega_1 = \Omega_A$ for spin A and at the point with $\omega_1 = \omega_2 = \Omega_X$ for spin X.

The third term in (19) describes the out-of-phase magnetization of spin A, which is precessing at frequencies $\Omega_X \pm \pi J_{AX}$. The center of the doublet of spin A is at the point $\omega_1 = \Omega_X, \omega_2 = \Omega_A$, which does not lie on the diagonal. The fourth term corresponds to a doublet of spin X, whose components precess at the frequencies $\Omega_A \pm \pi J_{AX}$; the center of the doublet is at the point $\omega_1 = \Omega_A, \omega_2 = \Omega_X$. Doublets which do not lie near the diagonal, $\omega_1 = \omega_2$, are also called "cross peaks."

The COSY experiment is performed twice in order to detect both the s_x and x_y components of the NMR signal: first with a pulse train $\pi/2(x) - t_1 - \pi/2(x)$ and then with

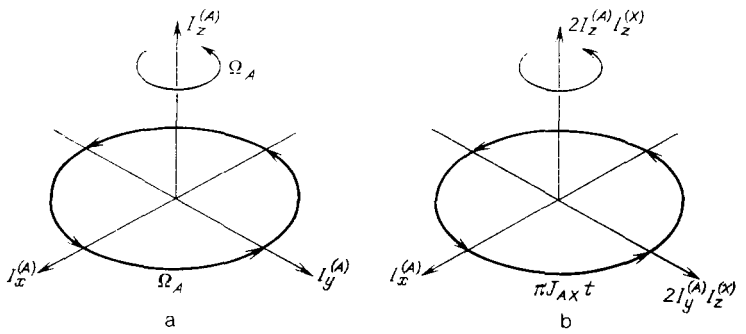

FIG. 6. Vector model of the evolution of spins in a system of two like spins A, X (e.g. protons) which are coupled. a—Under the influence of a chemical-shift effect; b—under the influence of a scalar coupling J_{AX}.

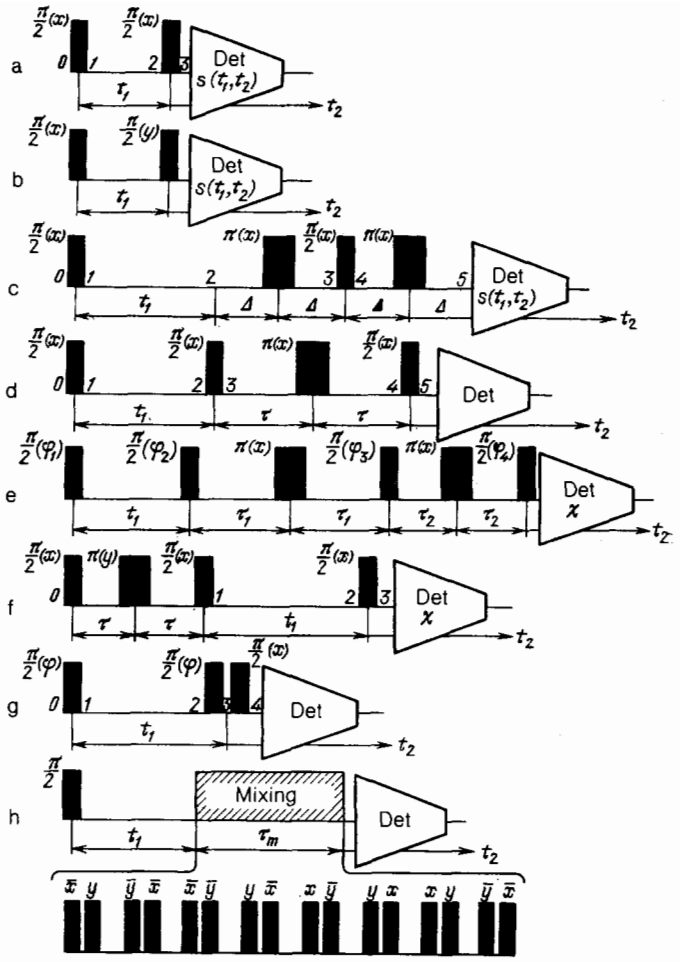

FIG. 7. Trains of rf pulses used in various versions of 2D COSY spectroscopy. a—Traditional 2D COSY with two $\pi/2$ rf field pulses (x, x experiment); b—x, y experiment in 2D COSY; c—SUPER COSY; d—relayed COSY (RCOSY); e—two-step RCOSY; f—two-quantum 2D COSY for spins A, X; g—COSY ⊕ multiquantum filter; h—isotropic mixing.

a pulse train $\pi/2(x) - t_1 - \pi/2\ (y)$ (Fig. 7b). In the first case, the second $\pi/2(x)$ pulse leaves the x component of the magnetization vector in the xy plane, while the y component is rotated to the z axis and is rendered unobservable. In the second case, the y component of the magnetization vector is left transverse in the xy plane.

In order to intensify the cross peaks corresponding to remote couplings of spins, whose intensity increases over time in accordance with $\sin \pi J_{AX} t_1$ [see (19)], time delays are introduced in the program of the COSY experiment both in the evolution stage (t_1) and after the second $\pi/2$ pulse, before the beginning of the detection of the NMR signal, depending on t_2 (Refs. 36 and 37). For an increased intensity of the doublets in the cross peaks, the latter are converted from the out-of-phase mode into the in-phase made by a train of rf SUPER COSY pulses[17,18] (Fig. 7c). The doublets on the diagonal are sent into the out-of-phase mode. If $\Delta = (4J_{AX})^{-1}$, the spin system AX at point 5 is in the state

$$\sigma_5 = (I_x^{(X)} \sin \Omega_A t_1 + I_x^{(A)} \sin \Omega_X t_1) \cos \pi J_{AX} t_1 - (2I_y^{(A)} I_z^{(X)} \sin \Omega_A t_1 + 2I_z^{(A)} I_y^{(X)} \sin \Omega_X t_1) \sin \pi J_{AX} t_1. \quad (20)$$

It can be seen from (20) that the cross peaks described by the first two terms in (2) have an in-phase magnetization and are in the dispersive mode. To put it into the absorbing mode, the phase of the reference signal in the receiver is changed by 90°, and the signal s_x is detected. The cross peaks in a SUPER COSY experiment are more intense than those in the traditional COSY arrangement (Fig. 8c), and we can clearly see cross peaks which are near the diagonal, $\omega_1 = \omega_2$. It thus becomes possible to observe remote spin couplings.

3.2. Relayed shift correlation spectroscopy (2D RCOSY). In shift correlation spectroscopy (2D COSY), the transfer of magnetization occurs only between spins which are cou-

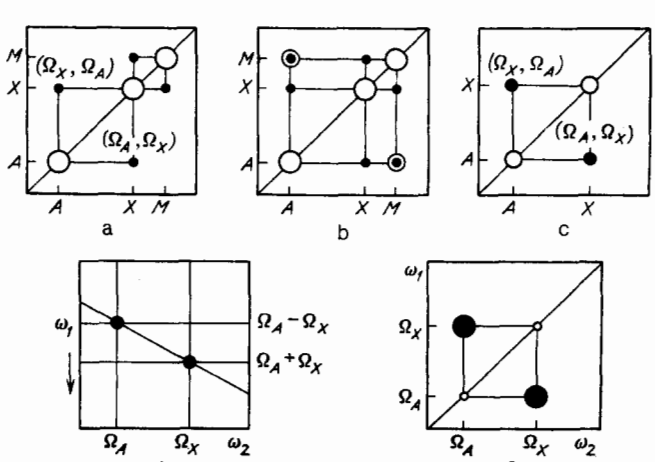

FIG. 8. Structures of the spectra in various versions of 2D COSY. a—Traditional 2D COSY spectrum; b—2D RCOSY; c—SUPER COSY; d—DQ COSY; e—TOCSY.

pled by a scalar coupling with $J \neq 0$. In relayed shift correlation spectroscopy (2D RCOSY) the magnetization is transferred between spins which are not directly coupled to each other, although each is coupled with a third spin (the "partner"). The transfer of magnetization is carried out in a relay fashion by means of a train of rf pulses which contains three $\pi/2$ pulses and one refocusing π pulse[19-22] (Fig. 7d). The first two $\pi/2$ pulses (2D COSY) initiate a transfer of magnetization between two directly coupled spins, while the refocusing π pulse eliminates the effect of the chemical shifts during the time interval between the second and third $\pi/2$ pulses. The third $\pi/2$ pulse initiates a transfer of magnetization to the third spin, the signal from which is detected immediately after the third $\pi/2$ pulse. In order to eliminate undesirable axial peaks and the Overhauser effect, the phases of the three $\pi/2$ pulses are alternated in accordance with[22]

$$\varphi_1 \rightarrow x, x, x, x,$$
$$\varphi_2 \rightarrow x, x, -x, -x,$$
$$\varphi_3 \rightarrow x, -x, x, -x.$$

The mechanism for the influence of the relayed transfer of magnetization can be explained using the example of three spins, *AXM*, in which spins *A* and *M* are not directly coupled[4,29] ($J_{AM} = 0$). The first $\pi/2(x)$ pulse creates a transverse magnetization ($-I_y^{(A)}$) of spin *A*. Under the influence of the chemical-shift effect (Ω) and the scalar spin-spin coupling (J_{AX}) the transverse magnetization of spin *A* evolves between the first and second $\pi/2$ rf pulses in accordance with

$$I_y^{(A)} \xrightarrow{\Omega_A t_1 I_z^{(A)} + 2\pi J_{AX} I_z^{(A)} I_z^{(X)} t_1} (-I_y^{(A)} \cos \Omega_A t_1 + I_x^{(X)} \sin \Omega_A t_1) \cos \pi J_{AX} t_1 + 2 (I_x^{(A)} \cos \Omega_A t_1 + I_y^{(A)} \sin \Omega_A t_1) I_z^{(X)} \sin \pi J_{AX} t_1. \quad (21)$$

The second $\pi/2(x)$ pulse at the end of the evolution stage converts the out-of-phase magnetization of spin *A*, described by the second term in (21), in accordance with

$$I_z^{(X)} (I_x^{(A)} \cos \Omega_A t_1 + I_y^{(A)} \sin \Omega_A t_1) \xrightarrow{\pi/2(I_x^{(A)} + I_x^{(X)})} - I_y^{(X)} (I_x^{(A)} \cos \Omega_A t_1 + I_z^{(A)} \sin \Omega_A t_1). \quad (22)$$

The first term on the right side of (22), $I_x^{(A)} I_y^{(X)}$, contains a two-quantum coherence (DQC) and a zero-quantum coherence (ZQC), which cannot contribute to the transfer of magnetization from spin *A* to spin *M*. The second term in (22) represents the *y* magnetization of *X* which was transferred from *A*. It is out of phase with respect to the magnetization of *A* and in phase with respect to that of *M*.

The π pulse at the center of the evolution stage eliminates the chemical-shift effect, while the second term in (22) evolves in accordance with

$$2I_z^{(A)} I_y^{(X)} \xrightarrow{2\pi J_{AX} I_z^{(A)} I_z^{(X)} \tau + 2\pi J_{XM} I_z^{(X)} I_z^{(M)}} - I_x^{(X)} \sin \pi J_{AX} \tau \cdot \cos \pi J_{XM} \tau + 2I_z^{(A)} I_y^{(X)} \cos \pi J_{AX} \tau \cdot \cos \pi J_{XM} \tau - 4I_z^{(A)} I_x^{(X)} I_z^{(M)} \cos \pi J_{AX} \tau \cdot \sin \pi J_{XM} \tau - 2I_y^{(X)} I_z^{(M)} \sin \pi J_{AX} \tau \cdot \sin \pi J_{XM} \tau. \quad (23)$$

The first term in (23) corresponds to the *x* magnetization of *X*, and it does not change after the $\pi/2(x)$ mixing pulse. A cross peak *A*,*X* arises in the 2D spectrum in the form of a doublet whose components are in phase along the ω_2 axis and out of phase along the ω_1 axis. The second term in (23), which goes into the state $-I_z^{(X)} I_y^{(A)}$, initiates a transfer of magnetization from *A* to *X* and then to *A*. Diagonal peaks appear in the 2D spectrum. The third term in (23), $I_x^{(X)} I_z^{(A)} I_z^{(M)}$, converts into a three-quantum coherence, which cannot contribute to the 2D spectrum. Only the fourth term in (23), $I_y^{(X)} I_z^{(M)}$, converts into an out-of-phase magnetization of spin *M*: $[-I_z^{(X)} I_y^{(M)}]$. After an alternation of the phases of the rf pulses, φ_1 and φ_2, and also of the phase of the reference signal in the receiver, χ, in accordance with

$$\varphi_1 \rightarrow x, x, y, y, -x, -x, -y, -y,$$
$$\varphi_2 \rightarrow x, -x, y, -y, -x, x, -y, y,$$
$$\chi \rightarrow + + - - + + - -$$

an NMR signal of the following type arises:

$$s_{AM} (t_1, t_2) = -i \sin \pi J_{AX} \tau \cdot \sin \pi J_{XM} \tau \times \sin \pi J_{AX} t_1 \cdot \sin \pi J_{XM} t_1 \times \exp (-i\Omega_A t_1) \cdot \exp (+ i\Omega_M t_2). \quad (24)$$

In order to suppress artifacts, the eight-cycle alternation of the phases φ_1, φ_2 is repeated four times; the phases of all the rf pulses and the phase χ are shifted through an angle of 90° in each case.

The relay chain of magnetization transfer can be put in a two-step form, $A \rightarrow X \rightarrow M \rightarrow N$, if an additional π pulse and a $\pi/2$ pulse of the rf field are introduced in the RCOSY train.[22] Figure 8, a and b, shows the structure of typical 2D COSY and 2D RCOSY spectra.

3.3. Multiquantum spectroscopy (MQS). There are no diagonal peaks in multiquantum spectra. This circumstance substantially simplifies the deciphering of the NMR spectra of large molecules and also the acquisition of data on the relative arrangement of spins which are not coupled by a mutually direct scalar coupling but are part of a branched chain of spin couplings in a molecule. Because of these properties, MQS serves as a supplement to COSY and RCOSY. Figure 7f shows the train of rf pulses used to obtain multiquantum spectra.[24-27] The exciting sandwich of $[\pi/2(x) - \tau - \pi(y) - \tau - \pi/2(x)]$ rf field pulses creates a multiquantum coherence. Under the influence of the scalar spin-spin coupling in a system of two spins, a state of the following form arises at the beginning of the evolution stage[4]:

$$\sigma_1 (\varphi = 0) = (I_z^{(A)} + I_z^{(X)}) \cos \pi J_{AX} 2\tau + (2I_x^{(A)} I_y^{(X)} + 2I_y^{(A)} I_x^{(X)}) \sin \pi J_{AX} 2\tau, \quad (25)$$

where the second term describes a purely two-quantum coherence. In the particular case of a system consisting of two spins ($p_{max} = 2$) the phase shift of the rf pulses is alternated in accordance with $\varphi = k\,2\pi/4$, $k = 0,1,2,3$. For $k = 0$ and 2 the DQCs are identical, while for $k = 1$ or 3 the DQCs have opposite signs. In the evolution stage, of duration t_1, the DQC is not affected by the J coupling between spins. Accordingly, the state

$$\sigma_2 = [(2I_x^{(A)}I_y^{(X)} + 2I_y^{(A)}I_x^{(X)})\cos(\Omega_A + \Omega_X)t_1 - (2I_x^{(A)}I_x^{(X)} - 2I_y^{(A)}I_y^{(X)})\sin(\Omega_A + \Omega_X)t_1] \times \sin(\pi J_{AX}\cdot 2\tau) \quad (26)$$

arises at the end of the evolution stage. After the mixing $\pi/2$ pulse, only the first term goes into an observable magnetization. At point 3, a state

$$\sigma_3^{obs} = (2I_x^{(A)}I_z^{(X)} + 2I_z^{(A)}I_x^{(X)})\cos(\Omega_A + \Omega_X)t_1 \times \sin(\pi J_{AX}\cdot 2\tau) \quad (27)$$

arises; it corresponds to an out-of-phase magnetization of spins A and X. Two out-of-phase doublets appear at points $\omega_2 = \Omega_A$ and $\omega_2 = \Omega_X$ in the 2D spectrum of MQC. There are no diagonal peaks. To determine the sign of the two-quantum precession, a β pulse with $\beta < \pi/2$ radians is used as the mixing pulse.[4,24] As a result, the first and second terms go into the observable one-quantum magnetization.

The cross peaks in the DQ COSY spectra[39] which stem from the scalar coupling of spins A and X at the frequencies of the chemical shifts, Ω_A and Ω_X, are found in the 2D spectrum $S(\omega_1,\omega_2)$ at the points with the coordinates $(\Omega_A + \Omega_X,\Omega_A)$ and $(\Omega_A + \Omega_X,\Omega_X)$, while in a traditional 2D COSY spectrum the same cross peaks are at the points with the coordinates (Ω_X,Ω_A) and (Ω_A,Ω_X).

In order to retain the two-quantum coherence DQC, while eliminating the signals from the zero-quantum coherence ZQC and the one-quantum coherence 1QC, the phase of the readout pulse, $\alpha(\psi)$, and of the reference signal in the receiver, χ, are alternated in accordance with the program[32]

$$\alpha \to x,\ y,\ -x,\ -y,$$
$$\chi \to x,\ -y,\ -x,\ y.$$

The undesirable coherence has been suppressed by a coefficient as high as[25] 1000:1.

The quadratic detection in DQS can be replaced by two experiments, which are carried out for each t_1; a 45° phase shift is introduced in the second experiment, at the end of the evolution stage.[47]

In order to obtain simple and easily decipherable DQS in systems consisting of many interacting spins, e.g., protons, measurements are carried out in which the rf pulse is rotated through $\alpha = 135°$ instead of $\alpha = 90°$, as in traditional DQS. Under these conditions the transfer of coherence to the passive spin (X) is reduced by a factor of 25, while the transfer of coherence to the spin which is not actively coupled (A and M) is reduced by a factor of only four. The transfer of coherence to the spins which are actively coupled is also reduced by a factor of 25. The result is a substantial decrease in the number of cross peaks which are observed. The signs of the coupling constants J_{AX}, J_{AM}, and J_{MX} are determined from the slope of the 2D multiplets.

Two-quantum spectroscopy, DQ COSY, separates the contributions of the spins which are and which are not coupled directly. The same result can be achieved by the method of polarization transfer between coupled spins,[58] in which a multiquantum coherence is not produced.

The multiquantum spectra in solids consist of very broad peaks. It was shown in Ref. 28, however, that the situation can be improved substantially by fixing the duration of the evolution stage, t_1, and repeating the experiments, in each case incrementing either the phase of the rf pulse, $\varphi = n\delta\tau$, or the frequency detuning $\Delta\omega = n\delta\omega$, where $n = 0, \pm 1, \pm 2, \ldots$. The NMR spectrum is detected at a fixed t_2^{fixed}. If a high sensitivity and narrow spectral lines are to be achieved, t_2^{fixed} must be quite small.

3.4. COSY ⊕ multiquantum filter (DQF COSY) The transfer of coherence between coupled spins and those that are not directly coupled depends differently on the rotation angle β of the mixing pulse. By carrying out experiments with different values of β, we can thus simplify the 2D COSY spectra substantially. For this purpose, one uses a train of three rf pulses of the type[30–32,54,55] (Fig. 7g)

$$\frac{\pi}{2}(\varphi) - t_1 - \frac{\pi}{2}(\varphi)\ \frac{\pi}{2}(x) - \text{detection based on } t_2.$$

The phase φ is alternated in order to bring out the purely two-quantum coherence between the second and third rf pulses. At point 3 after the second rf pulse, the system of the two spins A,X is in a state in which the multiquantum coherence can be represented as linear combinations of purely zero-quantum coherence ZQC and a purely two-quantum coherence DQC. As a result of the alternation of phases of the rf pulses, there is an averaging of the longitudinal magnetization, of the zero-quantum coherence ZQC, and of the out-of-phase one-quantum coherence. All that is left is the purely two-quantum coherence DQC:

$$\sigma_3^{DQC} = \left[\tfrac{1}{2}(2I_x^{(A)}I_y^{(X)} + 2I_y^{(A)}I_x^{(X)})\cos\Omega_A t_1 + \tfrac{1}{2}(2I_x^{(A)}I_y^{(X)} + 2I_y^{(A)}I_x^{(X)})\cos\Omega_X t_1\right] \times \sin\pi J_{AX}t_1. \quad (28)$$

After the third $\pi/2(x)$ pulse, a one-quantum magnetization arises:

$$\sigma_4^{obs} = \left[\tfrac{1}{2}(2I_x^{(A)}I_z^{(X)} + 2I_z^{(A)}I_x^{(X)})\cos\Omega_A t_1 + \tfrac{1}{2}(2I_x^{(A)}I_z^{(X)} + 2I_z^{(A)}I_x^{(X)}) \times \sin\Omega_X t_1\right]\sin\pi J_{AX}t_1. \quad (29)$$

The first and fourth terms in (29) correspond to diagonal peaks in the form of out-of-phase doublets along the ω_1 and ω_2 axes. There are no singlet components in this spectrum. In cases in which the width of a spectral ine is comparable to J, these doublets are reduced in intensity to the same extent as the cross peaks are. The second and third terms in (29) describe cross peaks which are distinguished from the cross peaks in COSY by intensities which are only half as high.[35]

A distinctive feature of traditional COSY is that the components of the cross peaks have opposite signs. The method of isotropic mixing is used to eliminate this disad-

vantage and to set the stage for the appearance of cross peaks from spins which are not coupled directly with each other, as in relayed COSY.[33] In addition to the second (mixing) rf pulse, one uses repeated symmetric trains of rf pulses, e.g., consisting of four $\pi(x)$ pulses or cycles of 16 pulses of the type $(-x,y;\ -y,-x;\ -x-y;\ -x;\ x,-y;\ y,x;\ x,y;\ -y,x)$. In this way one achieves a symmetric mixing; after this mixing, nonzero components of the following types remain in the A,X spin system: $I_x^{(A)}, I_x^{(A)}, I_x^{(A)}I_x^{(X)}$ and $I_y^{(A)}I_z^{(X)} - I_z^{(A)}I_y^{(X)}$. At a certain fixed time of isotropic mixing, τ_m, the COSY spectrum now contains in-phase signals in the absorbing mode, and the out-of-phase signals due to the component $I_y^{(A)}I_z^{(X)} - I_z^{(A)}I_y^{(X)}$ are in the dispersive mode. The in-phase signals do not change sign as a function of τ_m, while the out-of-phase signals do. In order to eliminate the out-of-phase components, the COSY spectra obtained at several (e.g., eight) different values of τ_m are averaged. In the method of isotropic mixing one obtains cross peaks not only for spins which are coupled directly with each other but also for spins which are not. For this reason, this method has been labeled "total-correlation spectroscopy" (TOCSY)[33] (Fig. 8d).

In shift correlation spectroscopy in which the spin echo is detected (SECSY),[16,40,42,53,66] the spin-echo signal is detected after the second (mixing) $\pi/2(x)$ pulse, which is applied at the center of the evolution stage, t_1. The COSY and SECSY spectra are related by[16]

$$S^{\mathrm{COSY}}(\omega_1, \omega_2) = \frac{1}{2} S^{\mathrm{SECSY}}\left(\frac{\omega_1 + \omega_2}{2},\ \omega_2\right). \qquad (30)$$

In traditional COSY with a $\pi/2(x) - \pi/2(x)$ pulse train, peaks arise at both positive and negative frequencies ω_1: $P(\omega_1,\omega_2)$ peaks, or antiecho signals, and $N(-\omega_1,\omega_2)$ peaks or echo signals.[15] These peaks go into corresponding peaks in the SECSY spectrum at the sum frequency, $P'((\omega_2+\omega_1)/2, \omega_2)$, and at the difference frequency, $N'((\omega_2-\omega_1)/2, \omega_2)$.

3.5. 2D J spectra. The multiplets caused by J couplings are seen in traditional 1D spectroscopy as spectral lines which are degenerate with respect to J. In the 2D spectra, this degeneracy is lifted, and each multiplet is rotated 45° or 90° around its own center. To record a 2D J spectrum, one uses a train of two pulses[43,64] (Fig. 9a). The first (nonselective) $\pi/2$ pulse creates a transverse magnetization and initiates a precession of the spins under the influence of the chemical shifts Ω and a separation of the components of the multiplet from each other under the influence of the scalar spin-spin coupling J. After the π pulse, which is applied at the center of the evolution stage, t_1, the effect of the chemical shifts is refocused, while the components of the J multiplets continue to separate from each other. The detection of the NMR signal as a function of the time t_2 is begun at the time $t = t_1$. Since the J coupling is present both in the evolution stage and in the detection stage, the components of the multiplets in the 2D J spectrum are spread out at an angle of 45° with respect to the $\omega_1 = \Omega$ axis. The values of J are plotted along the ω_2 axis. A spectral line in a 2D J spectrum consists of a mixture of the absorbing mode and the dispersive mode; the admixture of dispersive components greatly reduces the resolution in the J spectra. Accordingly, the 2D J spectra are usually presented as power spectra, i.e., in the absolute-value mode.[62,59,68]

To improve the resolution in the 2D J spectra, the detection of the signal $s(t_1, t_2)$ is begun immediately after the π rf field pulse[71] (Fig. 9b). In contrast with the train of rf pulses in Fig. 9a, the evolution stage in this case terminates at the time at which the π pulse is applied. Consequently, the chemical shifts (Ω) and the spin-spin coupling (J) contribute to the signal in both the evolution stage and the detection stage. An overlap of the 2D J spectra occurs; it can be prevented by changing the irradiation program, in precisely the same way as in the COSY-FOCSY experiment.[16,63] A 2D J-FOCSY spectrum is formed with a resolution and a sensitivity higher than in a conventional 2D J spectrum.

In order to suppress artifacts in the 2D J spectra, the phase (φ_1) of the $\pi/2$ pulse, the phase (φ_2) of the π pulse, and also the phase (χ) of the reference signal in the receiver are alternated in accordance with the following "EXORCYCLE" scheme[72]:

$$\varphi_1 \to 0,\ 0,\ 0,\ 0,$$
$$\varphi_2 \to 0,\ 90°,\ 180°,\ 270°,$$
$$\chi \to 0,\ 180°,\ 0,\ 180°.$$

3.6. Spectroscopy based on the Overhauser effect (NOESY). At thermal equilibrium, the energy levels of a spin system are filled in accordance with a Boltzmann distribu-

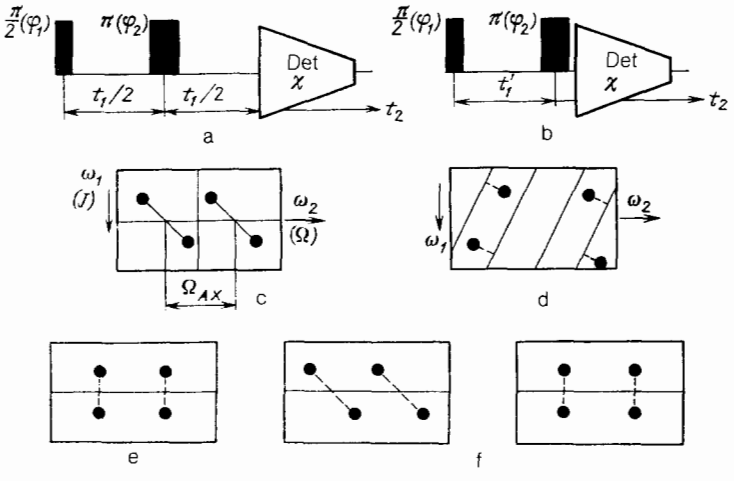

FIG. 9. Train of rf pulses used in obtaining 2D J spectra; structure of the J spectra. a—Conventional train; b—train for a FOCSY 2D J spectrum; c—conventional J spectrum; d—initial FOCSY spectrum; e—J spectrum after the slope has been eliminated; f—the same, for a FOCSY J spectrum.

tion. If a resonance line of spin A of a system of interacting spins A, X is selectively irradiated, however, the intensity of the resonance line of spin X will change (the Overhauser effect). This difference will increase as X moves closer to A. The rate of change of the NOE effect in time is inversely proportional to the sixth power of the distance between spins A and X. From the difference between the intensities of the resonance line of spin X which results from the selective excitation of spin A one can draw conclusions about the spatial proximity of A and X (Ref. 45). The Overhauser effect, which is caused by a dipole-dipole interaction of spins A and X, consists of two processes: 1) a pure change in the intensity of the observed spectral line and 2) a redistribution of the intensities of the spectral lines within a spin multiplet. The process of magnetization transfer under the influence of the Overhauser effect is incoherent by virtue of its very nature, and it is difficult to distinguish from a chemical-exchange effect. The same train of three pulses is used to study either of these phenomena[46-48] (Fig. 10a). The first (nonselective) $\pi/2$ pulse creates a transverse magnetization. The second $\pi/2$ pulse is a mixing pulse. In the mixing stage, of duration τ_m, both a cross relaxation and a chemical exchange occur. The NMR signal is detected after the third $\pi/2$ pulse. In the mixing stage, τ_m, it is necessary to distinguish the longitudinal magnetization by suppressing all the transverse coherences with $p = 1, 2, 3,...$ and the zero-quantum coherence (with $p = 0$). The latter has the same response as the longitudinal magnetization to phase shifts of the rf fields. If all the components of the transverse magnetization are omitted, the A, X spin system at point 3 will be in the following state after the second $\pi/2$ pulse at the beginning of the mixing stage[4]:

$$\sigma_3 = (-I_z^{(A)} \cos \Omega_A t_1 - I_z^{(X)} \cos \Omega_X t_1) \cos \pi J_{AX} t_1 + (I_y^{(A)} I_x^{(X)} - I_x^{(A)} I_y^{(X)}) (\cos \Omega_X t_1 - \cos \Omega_A t_1) \times \sin \pi J_{AX} t_1. \quad (31)$$

Taking account of the nature of the evolution of zero-quantum coherence, ZQC, and noting that the components of the longitudinal magnetization are mixed by chemical exchange and cross relaxation, we find that the observable magnetization after the third $\pi/2$ pulse at point 5 is

$$\sigma_5^{\text{набл}} = (I_y^{(A)} a_{AA} \cos \Omega_A t_1 + I_y^{(X)} a_{XX} \cos \Omega_X t_1 + I_y^{(A)} a_{XA} \cos \Omega_X t_1 + I_y^{(X)} a_{AX} \cos \Omega_A t_1) \cos \pi J_{AX} t_1 + (I_z^{(A)} I_x^{(X)} - I_x^{(A)} I_z^{(X)}) \cos (\Omega_A - \Omega_X) \tau_m \times (\cos \Omega_X t_1 - \cos \Omega_A t_1) \sin \pi J_{AX} t_1. \quad (32)$$

In the case of symmetric exchange the mixing coefficients are

$$a_{AA} = a_{XX} = \frac{1}{2} \exp(-R_1 \tau_m) [1 + \exp(-2\varkappa \tau_m)],$$
$$a_{AX} = a_{XA} = \frac{1}{2} \exp(-R_1 \tau_m) [1 - \exp(-2\varkappa \tau_m)], \quad (33)$$

where R_1 is the spin-lattice relaxation rate, and $\varkappa$ is the exchange constant. It can be seen from (32) that the diagonal peaks in the NOESY spectrum correspond to mixing coefficients α_{AA} and α_{XX} and that the exchange cross peaks are described by mixing coefficients α_{AX} and α_{XA} and are in phase with the J_{AX} peaks. In addition, there are out-of-phase

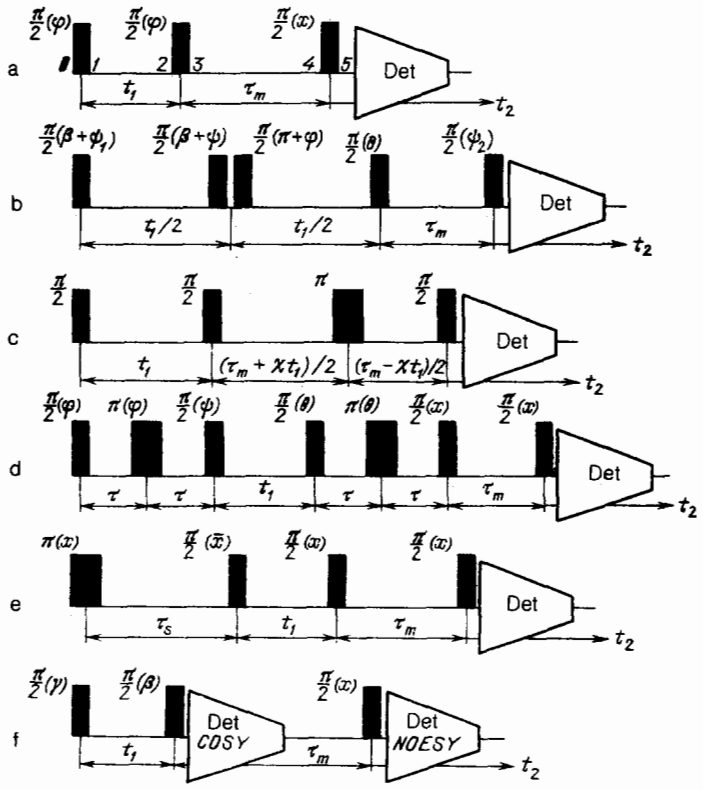

FIG. 10. Trains of rf pulses used in NOESY spectroscopy. a—Conventional train; b—NOESY with time reversal; c—scheme for separating NOE from J cross peaks; d—DQ NOESY; e—SKEWSY; f—COSY ⊕ NOESY or COCONOSY.

diagonal and cross peaks from the zero-quantum coherence, ZQC, in the NOESY spectrum.

Figure 11a shows a typical NOE spectrum. Peak A is due to a dipole-dipole coupling with peak C, while peak B is related to peaks D and E simultaneously. Similar effects arise from chemical exchange.[50]

If the time τ_m is varied systematically, the resulting data form a 3D NMR signal $s(t_1,t_2;\tau_m)$. After 2D Fourier transforms in t_1 and t_2 are taken, a 3D spectrum $S(\omega_1,\omega_2;\tau_m)$ arises. Incoherent effects cause $S(\omega_1,\omega_2;\tau_m)$ to vary smoothly as a function of τ_m, while coherent effects of a coherence transfer through J coupling, on the other hand, lead to rapidly oscillating changes in $S(\omega_1,\omega_2;\tau_m)$ as a function of τ_m. To suppress effects of ZQC, the value of τ_m is varied $\pm$ 10–20° for each t_1 and t_2, and the NMR signals are averaged. The phase coherence of the J correlation is disrupted, and as a result one is left with the effects of NOE and chemical exchange, which vary slowly τ_m. Finally, the NOESY spectrum also has some interference effects from the tranverse magnetization, which can be suppressed by simply alternating the phases of the rf pulses. The quadrature "image" along the ω_2 axis is eliminated in a corresponding way.

To distinguish the NOE effect from that of the J cross peaks, a refocusing π pulse is introduced in the irradiation scheme (Fig. 10c). This pulse is not applied at the center of the mixing period τ_m but shifted in a systematic way along with increments of t_1 (Ref. 56). A characteristic modulation of the NMR signal at the difference frequency (ZQC) and at the sum frequency (DQC) of the precession frequencies of spins A and X arises. After Fourier transforms are taken, the J cross peaks (and only these peaks!) shift a distance $\pm\chi(\omega_A-\omega_X)$ and $\pm\chi(\omega_A+\omega_X)$ from their original positions. In order to observe the Overhauser effect exclusively from close-lying spins A and X, the time τ_m is chosen to be quite small, e.g., 100 ms. At $\tau_m \sim 300$ ms, the Overhauser effect from very distant spins is also observed.

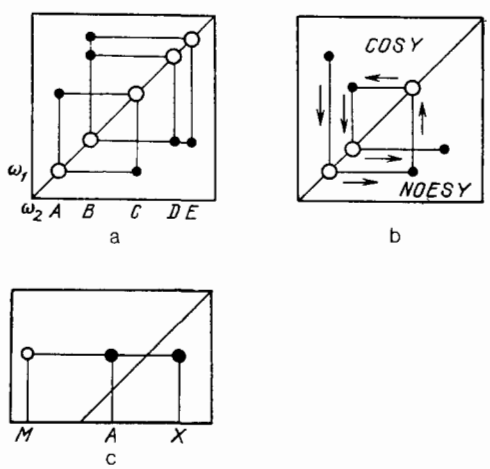

FIG. 11. Structure of NOESY spectra. a—Traditional NOESY spectrum, in which spin A is coupled in a dipole-dipole fashion with spin C, while spin B is dipole-dipole coupled with spins D and E; b—β-limaçon in a COSY ⊕ NOESY spectrum; c—DQ NOESY, in which the peaks stemming from J coupling are represented by filled circles, while the peak resulting from the incoherent dipole-dipole transfer of magnetization from spin A to spin M, which has no J coupling with either spin A or spin X, is shown by the open circle.

If the spin-lattice relaxation rate R_1 is small in comparison with the exchange constant $\varkappa$, differential exchange spectroscopy is used to eliminate the diagonal peaks, which are unrelated to exchange processes but which are predominant at short times t_1 (Ref. 51). The 2D spectrum found at $\tau_m = 0$ is subtracted from the 2D NOESY spectrum (Fig. 10a). For a higher efficiency of this method, the 2D spectra must be found in the pure mode. In this case, the amplitudes of the diagonal peaks which remain in the difference spectrum will be directly related to the diagonal elements of the exchange matrix.[32,33]

In an effort to suppress in this difference spectrum, the selective transfer of populations of energy levels, due to the different degrees of saturation of the sublevels of a multiplet, a method of preliminary irradiation of corresponding multiplets has been developed.[70] the two NMR signals which are obtained are summed in the data processing stage.

An interesting development of NOESY is SKEWSY spectroscopy.[44] The exchange rate and the cross relaxation rate in this case are measured in the absence of interference from a relayed transfer of magnetization. For this purpose, a perturbing π rf field pulse is introduced in the preparation stage in the NOESY scheme. The intensities of the peaks become redistributed, so the intensities of the cross peaks in the 2D SKEWSY spectrum can be greater than in conventional NOESY and greater than the intensities of the diagonal peaks.

For a systematic deciphering of the resonance lines in the 2D spectra, the COSY and NOESY spectra are placed side by side on a common plot: COSY in the upper left triangle and NOESY in the lower right triangle. Quite often the squence of J couplings on a composite 2D spectrum of this sort takes the form of a spiral (a β-limaçon[16]; Fig. 11b). A COSY ⊕ NOESY spectrum can be measured in a single experiment by recording the COSY spectrum and NOESY spectrum under identical conditions which do not introduce systematic errors.[59] Figure 10f shows a train of rf pulses in an experiment of this type. The first (nonselective) $\pi/2$ (γ) pulse creates a transverse magnetization and initiates the evolution of the magnetization over a time t_1. The second $\pi/2$ (β) pulse leaves the longitudinal component of the magnetization unchanged and initiates a transfer of this component of the magnetization among the spins which interact in a scalar fashion with each other. After the $\pi/2$ (β) pulse, while the magnetization components which remain in the x, y plane continue to precess at different frequencies ω_2, measurements of the 2D COSY spectrum are begun. After the $\pi/2$ (β) pulse, the perpendicular component of the transverse magnetization returns to the z axis and is subjected to cross relaxation or chemcial exchange effects during the mixing time τ_m. After the third $\pi/2$ (x) pulse, which transforms the longitudinal z component of the magnetization into a transverse component, the NOESY signal is detected. Axial peaks and also the multiquantum coherence of first, second, and third orders are eliminated from the COSY ⊕ NOESY spectrum through an appropriate alternation of the phases of the rf pulses. Four additional experiments are carried out in order to find a quadrature signal along the ω_2 axis. The number of independent experiments in Ref. 60 was 16.

The ambiguities which arise in the 2D NOESY spectrum due to the superposition of coherent (J-coupling) and incoherent dipole-dipole effects are eliminated in two-quan-

tum spectroscopy, DQ NOESY.[49] The first and second $\pi/2$ rf pulses are replaced by a sandwich of rf pules ($\pi/2$-τ-π-τ-$\pi/2$) (Fig. 10d). After the first sandwich of rf pulses has ended, an initial z magnetization arises from the two-quantum coherence, which is marked by the precession frequency of spins A, X, summed over the chemical shift. The second sandwich of rf pulses causes the transverse two-quantum coherence (DQC) to become a longitudinal magnetization. A cross relaxation develops in the mixing stage τ_m. The last $\pi/2$ rf pulse transforms the longitudinal magnetization into an observable transverse magnetization. The phases of the rf pulses are alternated in a definite way.[49] The DQ NOESY spectrum for a system of spins contains three types of peaks (Fig. 11c). Two of them, which are positioned symmetrically with respect to the diagonal, are caused by J couplings, while the third is at the frequency of spin M, which has no J coupling with either spin A or spin X. Spin M acquires a magnetization from A directly through the incoherent transfer mechanism by virtue of the dipole-dipole AM interaction.

An important shortcoming of NOESY spectroscopy is that the basic cross relaxation effect, which causes the changes in the intensities of the peaks of the observed spin, is accompanied by undesirable effects of a redistribution of intensity among the peaks within a given spin multiplet. This effect arises from a redistribution of the populations of the levels of spin system AX and is called "selective population transfer" (SPT).[57] To suppress the SPT effect in a two-spin system (AX), the frequency of the rf field is put exactly at the center of the corresponding doublet. In more-complex spin systems, however, the SPT effect cannot be eliminated in this simple way. A new method for eliminating the SPT effect was proposed in Ref. 57. That method is essentially one of analyzing the effect which arises in the case in which the $\pi/2$ readout pulse does not cause an exactly 90° rotation of the spin.[65] To explain this effect, we consider an out-of-phase perturbation of the level population, described by a state of two spins of the type $I_z^{(A)}I_z^{(X)}$. According to Ref. 69, the readout rf pulse can be thought of as a train of two semiselective rf pulses, of such a nature that the first acts only on spin A, and the second only on spin X.

In many of the methods described above for obtaining 2D NMR spectra, the phase of the rf pulses and the reference signal in the receiver are alternated. The phase alternation method, however, has its own shortcomings.[61] For example, it is not possible to distinguish a longitudinal magnetization from a zero-quantum coherence ZQC through an alternation of phases. It is in NOESY that this problem arises. For example, when a pulse train ($\pi/2$-t-$\pi/2$-t'-β) is used both the longitudinal magnetization existing before the β readout pulse and the zero-quantum coherence ZQC contribute to the signal which is detected. To distinguish between these two effects, one makes use of the dependence of the signal intensity on the spin-rotation angle β (Ref. 34).

3.7. Zero-quantum (ZQC) 2D spectra. By virtue of its physical nature, zero-quantum coherence ZQC contains information about spin-spin couplings. Attempts to make use of this property of ZQC in an actual experiment, however, run into two difficulties.[41] The pulse train $\pi/2\,(x)$-τ-$\pi(y)$-τ-$\pi/2(x)$ does not create a zero-quantum coherence ZQC in a weakly coupled system of like spins. On the other hand, the pulse train $\pi/2(x)$-τ-$\pi/2(x)$, although it does create a zero-quantum coherence ZQC, results in a situation in which the amplitudes of the individual zero-quantum transitions depend on both the spin-spin coupling and the chemical shifts. To excite a zero-quantum coherence ZQC in 2D NMR spectra, it is thus advisable to use an rf pulse train (Fig. 12) $\pi/2(x)$-τ-$\pi(y)$-τ-$\pi/4(y)$ (Ref. 41), which causes a fairly uniform excitation of zero-quantum transitions ZQC and in which the chemical-shift effect is suppressed by the π pulse. Afte the $\pi/4$ (y) pulse, a state $I_x^{(A)}I_z^{(A)}$ of the system of two spins goes into a state $I_z^{(A)}I_x^{(X)}$ with a zero-quantum coherence ZQC, while the magnetization of the uncoupled spins is not changed by the pulse. To suppress the undesirable signals and the polarization of the type $I_z^{(A)}I_z^{(X)}$ from bilinear effects, the phases of the four rf filed pulses at $t_1 = 0$ are alternated in accordance with

$$\varphi_1 \to x, x, x, x,\ \varphi_2 \to y, -y, y, -y,$$
$$\varphi_3 \to y, y, -y, -y, \qquad \varphi_4 \to y, y, y, y,$$
$$\chi \to x, x, -x, -x.$$

At the time $t_1 = 0$, a magnetic field pulse (12a) is applied and destroys the uniformity of the magnetic field.[41] However, we are left with an insignificant magnetization resulting from the imperfections in rf pulses.

As was noted in Ref. 34, in the case $\alpha < \pi/2$ the transfer of zero-quantum coherence ZQC to passive spins (Fig. 12b), which are not participating in the formation of the ZQC, is weakened, and the ZQC is reflected well in one version of the 2D spectrum. At short times τ, the correlations with large J are emphasized, while the couplings between remote spins are on the contrary, weakened. The correlation between the 2D ZQC peaks for $\alpha = \pi/2$ radians is represented by horizontal lines which run parallel to the ω_2 axis. For $\alpha = \pi/4$ radians, the correlation between peaks runs along the diagonal $(\omega_2, -2\omega_1)$.

3.8. 3D NMR spectra and ACCORDIAN spectra. Several factors make it necessary in NMR spectroscopy to record a three-dimensional (3D) signal $s(t_1,t_2,t_3)$, which depends on three time variables. The first factor is the desire to combine two methods of 2D spectroscopy in a single experiment. The effectiveness of that approach is demonstrated by the progress which has been achieved in joint measurements of the COSY ⊕ NOESY effects.[59,60] This experiment, however, is not three-dimensional in nature. The information which is recorded in the course of such an experiment consists of an ordered set of two (and only two!) NMR signals, $s_{\mathrm{COSY}}(t_1,t_2)$ and $s_{\mathrm{NOESY}}(t_1,t_2)$. A truly three-dimensional experiment may arise from a parallel combination of two

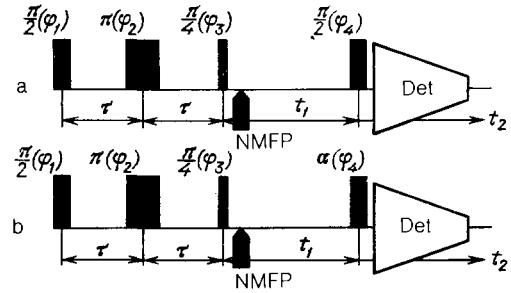

FIG. 12. Diagram of experiments with a zero-quantum coherence. a—With a detecting $\pi/2$ pulse; b—with a detecting α pulse, where $\alpha < \pi/2$. NMFP) Nonuniform magnetic field pulse.

methods of 2D spectroscopy, e.g., 2D COSY and 2D J spectroscopy.[66] The first of these methods yields the correlation between the chemical shifts of two coupled spins A, X; the second method forms the (Ω,J) spectra of the same spins. In a three-dimensional NMR signal $s(t_1,t_2,t_3)$ there is information on both the correlation of chemical shifts and the 2D J spectra. After three-dimensional Fourier transforms of the NMR signal $x(t_1,t_2,t_3)$ are taken, a 3D spectrum $S(\omega 1,\omega_2,\omega_3)$ arises in which the J spectra are separated in frequency by an amount determined by the chemical shift of the corresponding spin. In a 3D NMR spectrum we see all the multiplets, all the scalar couplings, and all the chemical shifts.

The need for recording 3D NMR signals arises in the most natural way in NOESY upon a variation of the duration of the mixing stage, τ_m (Ref. 68). In this case one detects NMR signals of the type $s(t_1,\tau_m,t_2)$, which is converted by two-dimensional Fourier transforms into a 3D spectrum $S(\omega_1,\tau_m,\omega_2)$. This natural generalization, however, requires a significant increase in the duration of the experiment, renders the 3D experiment extremely expensive and inaccessible for many research groups, and has the further disadvantage that possible variations in experimental conditions will lead to undesirable results.

The situation is different in NMR spectroscopy of the ACCORDION type,[67,68] in which a 3D data file is reduced to a 2D file. We can illustrate the working principle of ACCORDION spectroscopy with the example of 2D exchange NOESY spectroscopy, in which one uses a train of three $\pi/2$ rf field pulses. In conventional 2D NOESY the duration of the mixing stage, τ_m, remains constant, and the duration of the evolution stage is systematically changed. The NMR signals are detected as functions of the time (t_2) after the last $\pi/2$ pulse. In an ACCODION experiment, the duration of the mixing stage, τ_m, is changed at the same time (!) that the duration of the evolution stage, t_1, is changed:

$$\tau_m = kt_1. \tag{34}$$

Here a 3D experiment in which all the time variables t_1,t_2, and τ_m are changed is reduced to a 2D experiment. In the stage of Fourier transforms, relationship (34) between times τ_m and t_1 has the consequence that 1D Fourier transforms in t_1 are simultaneously ID Fourier transforms in τ_m. As a result of this sleight of hand, the frequency axes ω_1 and ω_m run parallel to each other, so the spectral range along the ω_m axis is shorter than that along the ω_1 axis by a factor of k. The frequency axes ω_1 and ω_2 have different physical meanings in an ACCORDION experiment.

Since the mixing coefficients α_{AA} and α_{AX} in a NOESY experiment depend on the time τ_m [see (33)], a 1D Fourier transform of the NMR signal along the time τ_m results in different spectral peaks along the ω_m axis:

$$a_{AA}(\tau_m) \rightarrow S_{AA}(\omega_m) = \frac{1}{2}\left[\frac{R_1}{R_1^2+\omega_m^2} + \frac{2\varkappa+R_1}{(2\varkappa+R_1)^2+(\omega_m)^2}\right] \tag{35}$$

for a diagonal peak and

$$a_{AX}(\tau_m) \rightarrow S_{AX}(\omega_m) = \frac{1}{2}\left[\frac{R_1}{R_1^2+\omega_m^2} - \frac{2\varkappa+R_1}{(2\varkappa+R_1)^2+(\omega_m)^2}\right] \tag{36}$$

for a cross peak.

It can be seen from (35) and (36) that a spectral line in a diagonal peak consists of the sum of the two Lorentzian lines. The width of the first of these lines is determined by the spin-lattice relaxation rate R_1, while the width of the second is determined by the sum $(2\varkappa + R_1)$, where $\varkappa$ is the exchange constant. A spectral line of a cross peak, which is the difference between the same Lorentzian lines, contains information about the exchange constant $\varkappa$ which can easily be extracted.

Finally, we take a look at the relationship between a 2D ACCORDION spectrum and a 3D NMR spectru. The data file of 2D spectra $S(\omega_1,\tau_m,\omega_2)$ with n values of the parameter τ_m is in the form of a stack of 2D spectra. After a discrete Fourier transform of the function $S(\omega_1,\tau_m,\tau_2)$ in τ_m, a stack of n 2D spectra $S(\omega_1,\tau_m,\omega_2)$ arises with a discrete parameter ω_m. We see that a 1D stack of 2D spectra is equivalent to the total 3D NMR spectrum and that the 2D ACCORDION spectrum in an oblique projection[38] of this 3D spectrum onto the ω_1 axis. The angle (ε) at which this oblique projection is made is determined unambiguously by the quantity k in (34):

$$\operatorname{tg}\varepsilon = k. \tag{37}$$

4. RENAISSANCE OF 1D NMR SPECTROSCOPY

The pronounced overlap of spectral lines in the 1D NMR spectra is eliminated in the 2D and 3D NMR spectroscopies described in the preceding sections of this review. The researcher thus gains access to information which makes it possible to decipher the structure of inorganic and organic molecules. While the corresponding evaluations of the structure of molecules were qualitative in the first stage of development of multidimensional method of NMR spectroscopy, advanced NMR-spectroscopy methods and equipment now make it possible to carry out a quantitative analysis of the structure of molecules. Shift correlation NMR spectroscopy (COSY) is used where it is necessary to evaluate the coupling constants J of spins which are directly coupled or to transfer coherence along a chain of coupled signs in a relay fashion (RCOSY). To obtain data on the relative spatial positions of spins one uses Overhauser-effect spectroscopy (NOESY). The method of 2D NMR spectroscopy has several important disadvantages. The primary disadvantage is that the time required for the measurements and for the processing of multidimensional NMR spectra is very long (~ 10 h or more), and a large digital memory is required for storing and converting the data. It is thus not surprising that researchers have always wanted to find appropriate equivalents of the methods of multidimensional NMR spectroscopy, especially for problems in which only partial information on the J couplings and the Overhauser effect would be sufficient. A solution has been found through the use of the method of selective excitation of spins.[73] For this purpose, the first (nonselective) $\pi/2$ (x) rf pulse is replaced by a selective $\pi/2$ pulse with a Gaussian envelope. The width of the excitation spectrum in the selective $\pi/2$ pulse is chosen so small that only transitions pertaining to one multiplet, e.g., those of spin X in a spin system A, M, X, are excited. The 1D NMR spectrum which is recorded will then not have multiplets of spins A and M. Figure 13a shows the program of an experi-

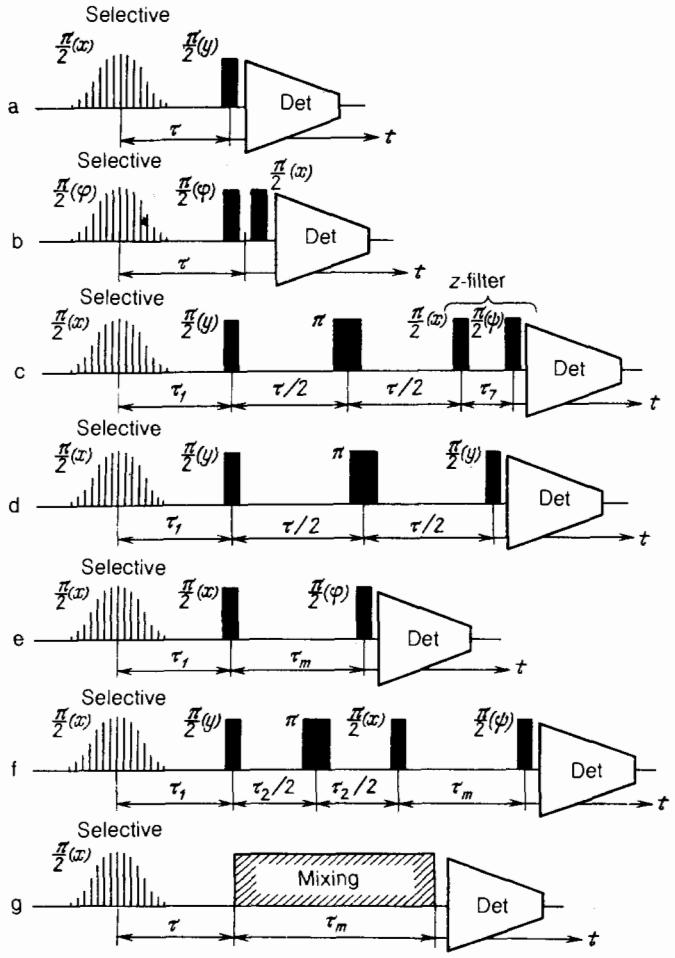

FIG. 13. Trains of rf pulses used in selective one-dimensional (1D) spectroscopies. a—Traditional 1D COSY; b—1D DQ COSY; c—1D COSY with a z-filter; d—1D RCOSY; e—Traditional 1D NOESY; f—1D relayed NOESY; g—1D TOCSY.

ment which is a 1D equivalent of a 2D COSY experiment (Fig. 7). Remarkably, with a short evolution stage τ (5 ms) the transfer of coherence described by the function $\sin\pi J\tau$ goes only to the nearest multiplet of spin M, which lies 0.35 md away from multiplet X in the spectrum. When the duration of the evolution stage is $\tau = 70$ ms, only the remote multiplet of spin A (0.8 md) is excited; the nearby multiplet is spin M is not excited ($\pi J\tau = \pi$). At an intermediate duration of the evolution stage, $\tau = 30$ ms, the magnetization is transferred to both the nearby multiplet of spin M and the remote multiplet of spin A. This result shows that in a one-dimensional 1D COSY experiment it is possible to achieve a twofold selectivity: in both Ω and J.

It has been verified experimentally[73] that in the case of a J-selective transfer of magnetization to an out-of-phase multiplet the center of the multiplet acquires zero intensity. This circumstance can be utilized to improve the accuracy of measurements of the coupling constant J between corresponding spins.

If a sample is irradiated simultaneously by pulses which constitute a combination 1D COSY $\oplus$ z-filter (Fig. 13c), the out-of-phase multiplet becomes an in-phase multiplet. The sum and difference of 1D spectra with out-of-phase and in-phase multiplets contain multiplets with half the number of components. From the shift of the centers of the "truncated" multiplets in the sum and difference spectra one can evaluate the constant of the active coupling.

The one-dimensional analog, 1D RCOSY, illustrated in Fig. 13e, with a relayed transfer of magnetization can be used to obtain 1D spectra of residues of individual amino acids.[73] Figures 13, b, d, f, and g, show the diagrams of 1D equivalents of several other experiments from 2D NMR spectroscopy.

Finally, Fig. 14 shows an example which demonstrates that the popularity of 1D spectroscopy is on the rise, rather than on the wane. This experiment involves a relayed transfer of magnetization[62] in which the pattern of nearby and remote couplings can be studied simultaneously. Selectivity is achieved in this experiment through the use of a train of weak rf field pulses (DANTE).[42] If the number of relay transfers is small, an experiment of this type can be carried out much more rapidly than the corresponding 2D experiment, but equivalent information will be obtained.

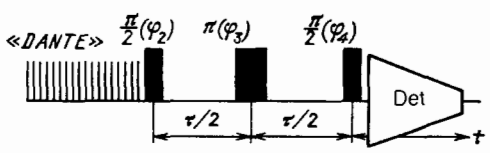

FIG. 14. Train of rf pulses in one-dimensional (1D) spectroscopy with a relayed transfer of magnetization.

5. CONCLUSION

We have examined methods of multipulse NMR spectroscopy, discussing them in this review for the particular case of a system consisting of two like (but not equivalent) nuclear spins. These methods were developed in order to simplify the process of interpreting complex *one-dimensional* NMR spectra. Today, in a new stage in the development of NMR technology, researchers are developing methods for simplifying *two-dimensional* NMR spectra. They are also developing algorithms for deciphering NMR spectra by computer. In the course of this development effort, the methods of COSY, RCOSY, MQS, NOESY, etc., remain the basic building blocks of the new structures. There is accordingly reason to believe that this review will remain useful for the foreseeable future (particularly for someone who is just beginning research in the field), as a general chart of the endless ocean of methods in NMR spectroscopy today.

[1]L. M. Lederman, [Russ. Transl. Vmirenauki. (1985), No. 1, p. 11].
[2]A. G. Lundin and E. I. Fedin, NMR Spectroscopy (In Russian), Nauka, M., 1986.
[3]L. M. Soroko, Nuclear-Magnetic-Resonance Subsurface Imaging (In Russian), Energoatomizdat, M., 1986.
[4]O. W. Sorensen, G. W. Eich, M. H. Levitt, G. Bodenhausen, and R. R. Ernst, Prog. Nucl. Magn. Reson. Spectrosc. **16**, 163 (1983).
[5]G. Bodenhausen, Prog. Nucl. Magn. Reson. Spectrosc. **14**, 137 (1981).
[6]R. M. Lynden-Bell, J. M. Bulsing, and D. M. Doddrell, J. Magn. Reson. **55**, 128 (1983).
[7]O. W. Sorensen, M. H. Levitt, and R. R. Ernst, J. Magn. Reson. **55**, 104 (1983).
[8]G. Bodenhausen, H. Kogler, and R. R. Ernst, J. Magn. Reson. **58**, 370 (1984).
[9]Yen Yu-Sze, and A. Pines, J. Chem. Phys. **78**, 3579 (1983).
[10]J. Baum, M. Munowitz, A. N. Garroway, and A. Pines, J. Chem. Phys. **83**, 2015 (1985).
[11]D. P. Weitekamp, Adv. Magn. Reson. **11**, 111 (1983).
[12]R. Freman, T. A. Frenkiel, and M. H. Levitt, J. Magn. Reson. **44**, 409 (1981).
[13]K. J. Packer and K. M. Wright, Mol. Phys. **50**, 797 (1983).
[14]W. P. Aue, E. Bartholdi, and R. R. Ernest, J. Chem. Phys. **64**, 2229 (1976).
[15]K. Nagayama, J. Magn. Reson. **66**, 240 (1986).
[16]K. Nagayama, Kumar Anil, K. Wuthrich, and R. R. Ernst, J. Magn. Reson. **40**, 321 (1980).
[17]Kumar Anil, R. V. Hosur, and K. Chandrasekhar, J. Magn. Reson. **60**, 143 (1984).
[18]R. V. Hosur, K. V. R. Chary, Kumar Anil, and G. Govil, J. Magn. Reson. **62**, 123 (1985).
[19]G. Eich, G. Bodenhausen, and R. R. Ernst, J. Am. Chem. Soc. **104**, 3731 (1982).
[20]P. H. Bolton, J. Magn. Reson. **48**, 336 (1982).
[21]P. H. Bolton and G. Bodenhausen, Chem. Phys. Lett. **89**, 139 (1982).
[22]G. Wagner, J. Magn. Reson. **55**, 151 (1983).
[23]Bax Ad, *Two-Dimensional Nuclear Magnetic Resonance in Liquids*, Delft Univ. Press, Dordrecht, Holland, 1982.
[24]T. H. Mareci and R. Freeman, J. Magn. Reson. **48**, 158 (1982).
[25]T. H. Mareci and R. Freeman, J. Magn. Reson. **51**, 531 (1983).
[26]M. A. Thomas and Kumar Anil, J. Magn. Reson. **54**, 319 (1983).
[27]M. Rance, O. W. Sorensen, W. Leupin, H. Kogler, K. Wuthrich, and R. R. Ernst, J. Magn. Reson. **61**, 67 (1985).
[28]S. Emid, Physica Ser. B + C **128**, 79 (1985).
[29]Bax Ad and G. Drobny, J. Magn. Reson. **61**, 79 (1985).
[30]U. Piantini, O. W. Sorensen, and R. R. Ernst, J. Am. Chem. Soc. **104**, 6800 (1982).
[31]G. Bodenhausen and Ch. M. Dobson, J. Magn. Reson. **44**, 212 (1981).
[32]Bax Ad, R. Freeman, and S. R. Kempsell, J. Am. Chem. Soc. **102**, 4849 (1980).
[33]L. Braunschweiler and R. R. Ernst, J. Magn. Reson. **53**, 521 (1983).
[34]L. Braunschweiler, G. Bodenhausen, and R. R. Ernst, Mol. Phys. **48**, 535 (1983).
[35]G. Otting and K. Wuthrich, J. Magn. Reson. **66**, 359 (1986).
[36]Bax Ad, and R. Freeman, J. Magn. Reson. **44**, 542 (1981).
[37]T. T. Nakashima and D. L. Rabenstrein, J. Magn. Reson. **66**, 157 (1986).
[38]P. Mansfield and A. A. Maudsley, J. Magn. Reson. **27**, 101 (1977).
[39]E. R. P. Zuiderwerg, J. Magn. Reson. **66**, 153 (1986).
[40]Kumar Anil, R. V. Hosur, K. Chandrasekhar, and N. Murali, J. Magn. Reson. **63**, 107 (1985).
[41]L. Muller, J. Magn. Reson. **59**, 326 (1984).
[42]G. A. Morris and R. Freeman, J. Magn. Reson. **29**, 433 (1978).
[43]R. Freeman and G. A. Morris, Bull. Magn. Reson. **1**, 5 (1980).
[44]J. Bremer, G. L. Mendz, and W. J. Moore, J. Am. Chem. Soc. **106**, 4691 (1984).
[45]J. Jeener, B. H. Meier, P. Bachman, and R. R. Ernst, J. Chem. Phys. **71**, 4546 (1979).
[46]S. Macura and R. R. Ernst, Mol. Phys. **41**, 95 (1980).
[47]Bax Ad, R. Freeman, T. A. Frenkiel, and M. H. Levitt, J. Magn. Reson. **43**, 478 (1981).
[48]Bax Ad, R. Freeman, and T. A. Frenkiel, J. Am. Chem. Soc. **103**, 2102 (1981).
[49]F. J. M. Van de Ven, C. A. G. Haasnoot, and C. W. Hilbers, J. Magn. Reson. **61**, 181 (1985).
[50]S. Macura, Y. Huang, D. Suter, and R. R. Ernst, J. Magn. Reson. **43**, 259 (1981).
[51]G. Bodenhausen and R. R. Ernst, Mol. Phys. **47**, 319 (1982).
[52]Bax Ad, A. F. Mehlkopf, and J. Smidt, J. Magn. Reson. **35**, 167 (1979).
[53]D. P. Weitekamp, J. R. Garbow, J. B. Murdoch, and A. Pines, J. Am. Chem. Soc. **103**, 3578 (1980).
[54]A. J. Shaka and R. Freeman, J. Magn. Reson. **51**, 169 (1983).
[55]S. Macura, K. Wuthrich, and R. R. Ernst, J. Magn. Reson. **47**, 351 (1982).
[56]S. Macura, K. Wuthrich, and R. R. Ernst, J. Magn. Reson. **46**, 269 (1982).
[57]A. Shaka, Ch. Bauer, and R. Freeman, J. Magn. Reson. **60**, 479 (1984).
[58]Ch. Dumoulin and E. A. Williams, J. Magn. Reson. **66**, 86 (1986).
[59]A. Z. Gurevich, I. L. Barsukov, A. S. Arseniev, and V. F. Bystrov, J. Magn. Reson. **56**, 471 (1984).
[60]C. A. G. Haasnoot, F. J. M. van de Ven, and C. W. Hilbers, J. Magn. Reson. **56**, 343 (1984).
[61]P. H. Bolton, J. Magn. Reson. **60**, 342 (1984).
[62]J. Santoro, M. Rico, and F. J. Bermejo, J. Magn. Reson. **67**, 1 (1986).
[63]M. A. Thomas and Kumar Anil, J. Magn. Reson. **56**, 479 (1984).
[64]L. D. Hall and S. Sukumar, J. Magn. Reson. **38**, 559 (1980).
[65]S. Schaublin, A. Hohener, and R. R. Ernst, J. Magn. Reson. **13**, 196 (1974).
[66]P. H. Bolton, J. Magn. Reson. **46**, 343 (1982).
[67]G. Bodenhausen and R. R. Ernst, J. Magn. Reson. **45**, 367 (1983).
[68]G. Bodenhausen and R. R. Ernst, Am. Chem. Soc. **104**, 1304 (1982).
[69]G. Bodenhausen and R. Freeman, J. Magn. Reson. **36**, 221 (1979).
[70]D. Neuhaus, J. Magn. Reson. **53**, 109 (1983).
[71]S. Macura and L. R. Brown, J. Magn. Reson. **53**, 529 (1983).
[72]G. Bodenhausen, R. Freeman, and D. L. Turner, J. Magn. Reson. **27**, 511 (1977).
[73]W. Bermel, H. Kessler, C. Griesinger, and H. Oschkinat, Bruker Rept. No. 1, 22 (1986).

Translated by Dave Parsons